

# Hydrological signatures describing the translation of climate seasonality into streamflow seasonality

Sebastian J. Gnann<sup>1</sup>, Nicholas J. K. Howden<sup>1</sup>, and Ross A. Woods<sup>1</sup>

<sup>1</sup>Department of Civil Engineering, University of Bristol, Bristol, UK

**Correspondence:** Sebastian Gnann (sebastian.gnann@bristol.ac.uk)

**Abstract.** Seasonality is ubiquitous in nature, and it is closely linked to water quality, ecology, hydrological extremes, and water resources management. Hydrological signatures aim at extracting information about certain aspects of hydrological behaviour. Commonly used seasonal hydro-climatological signatures consider climate or streamflow seasonality, but not how climate seasonality translates into streamflow seasonality. In order to analyse the translation of seasonal climate input (precipitation minus potential evapotranspiration) into seasonal catchment output (streamflow), we represent the two time series by their seasonal (annual) Fourier mode, i.e. by sine waves. A catchment alters the input sine wave by reducing its amplitude and by shifting its phase. We propose to use these quantities, the amplitude ratio and the phase shift, as seasonal hydrological signatures. We present analytical solutions describing the response of linear reservoirs to periodic forcing to interpret the seasonal signatures in terms of configurations of linear reservoirs. Using data from the UK and the US, we show that the seasonal signatures exhibit hydrologically interpretable patterns and that they are a function of both climate and catchment attributes. Wet, rather impermeable catchments hardly attenuate the seasonal climate input. Drier catchments, especially if underlain by a productive aquifer, strongly attenuate the input sine wave leading to phase shifts up to several months. As an example application, we test whether two commonly used hydrological models (IHACRES, GR4J) can reproduce the observed ranges of seasonal signatures in the UK. The results show that the seasonal signatures have the potential to be useful for catchment classification, for predictions in ungauged catchments, and to aid model building and evaluation. The use of potential evapotranspiration in the input restricts the applicability of the signatures to energy-limited (humid) catchments.

## 1 Introduction

The annual course of the earth around the sun leads to seasonal cycles in climate in many places. Seasonal patterns in precipitation, evapotranspiration, and snowfall, as well as the characteristics of the catchment a stream drains, often result in a distinct seasonal streamflow regime (Cayan et al., 1993; Regonda et al., 2005; Berghuijs et al., 2014). The seasonal flow regime is closely linked to water chemistry and water quality (DeWalle et al., 1997; Vega et al., 1998). Streamflow seasonality plays a crucial role for biological systems and ecosystems (Colwell, 1974; Poff et al., 1997; Poff and Zimmerman, 2010). Low flows are typically seasonal, and droughts – albeit a more general phenomenon than low flows – often occur during the low flow season and thus are to some degree predictable (Smakhtin, 2001; Peters et al., 2003). From a more applied point of view, the seasonal streamflow regime is crucial for water resources management, agriculture, and hydropower generation (Weingartner

et al., 2013; Laaha et al., 2013; Svensson, 2016; Harrigan et al., 2018b). This is reflected in the increased application and development of seasonal forecasting methods (Shi et al., 2008; Svensson, 2016; Harrigan et al., 2018b). In summary, for many applications the mean seasonal regime is of high importance and thus deserves attention.

30 In this work we focus on the average seasonal hydrological response of snow-free catchments. We do not focus, for instance, on the seasonality of events (e.g. storms), noting, however, that the seasonal water balance can have an impact at event scales (Berghuijs et al., 2014). In snow-free areas, the seasonality of the flow regime is primarily driven by the incoming forcing, that is, the seasonality of precipitation (water) and potential evapotranspiration (energy). Given a certain forcing, the flow regime of a catchment is determined by a catchment's form and function, that is, by how much water can infiltrate, how much water can be stored, and how slowly that water is being released. Since groundwater recharge and thus groundwater discharge is  
35 often very seasonal (Jasechko et al., 2014), many hydrogeological studies focus on seasonality, or more specifically on how seasonal recharge is propagated through an aquifer system (Townley, 1995; Erskine and Papaioannou, 1997; Peters et al., 2003; Oberghell et al., 2019). Slowly responding, groundwater-dominated catchments closely resemble the aquifer system feeding the stream. Understanding the seasonal streamflow regime is therefore particularly important for understanding slow (groundwater-driven) dynamics in catchments.

40 Different aspects of hydrological behaviour, such as streamflow seasonality, can be quantified by summarising metrics now mostly called hydrological signatures (McMillan et al., 2017). The use of such summarising metrics is not new, and they have been used extensively in ecohydrological studies (e.g. Clausen and Biggs, 2000; Olden and Poff, 2003) and hydrological studies (e.g. Jothityangkoon et al., 2001; Farmer et al., 2003). Hydrological signatures offer a way to quantify hydrologic similarity. This makes them useful for catchment classification (Wagener et al., 2007; Sawicz et al., 2011), for hydrological  
45 process exploration (McMillan et al., 2014), and for predictions in ungauged basins (Yadav et al., 2007; Hrachowitz et al., 2013; Westerberg et al., 2016). Hydrological signatures can also be used to guide diagnostic model evaluation (Gupta et al., 2008; Peel and Blöschl, 2011; Euser et al., 2013; Hrachowitz et al., 2014; Shafii and Tolson, 2015), as they offer a potentially more meaningful and fit-for-purpose alternative to the typically used statistical metrics such as the Nash-Sutcliffe efficiency (NSE; Nash and Sutcliffe, 1970) or the Kling-Gupta efficiency (KGE; Gupta et al., 2009).

50 There are many hydrological signatures and we therefore need guidelines for signature selection (McMillan et al., 2017; Addor et al., 2018). Some of these guidelines refer to more technical aspects: the uncertainty in a signature should not be larger within a catchment than between catchments (identifiability), a signature should be insensitive to the data sources (robustness), and a signature should be comparable across (heterogeneous) catchments (consistency; McMillan et al., 2017). When using combinations of signatures, the different signatures should also contain different information, i.e. they should not be redundant (Olden and Poff, 2003; Addor et al., 2018). From a more hydrological perspective, a signature should be meaningful at  
55 the relevant scale (representativeness) and a signature should relate to and increase our knowledge of hydrological function (discriminatory power; McMillan et al., 2017). Since (hydro-)climatic signatures such as the mean flow are already well understood, we should try to explain and use signatures that tell us more about catchment functioning (Addor et al., 2018), such as signatures that relate climate input to catchment output.

60 There is a multitude of hydrological signatures focusing on seasonality. Climate seasonality is accounted for by (hydro-  
)climatic signatures such as the (co-)seasonality of precipitation and potential evapotranspiration (Milly, 1994; Knoben et al.,  
2018). Streamflow seasonality can be characterised by the Pardé coefficients (Weingartner et al., 2013) or the regime curve,  
which is related to the slow flow component of the flow duration curve (FDC; Yokoo and Sivapalan, 2011). Seasonal signa-  
65 one-day maximum (or minimum; Richter et al., 1996). Seasonal streamflow signatures focusing on low flows are for example  
the seasonality index, which measures the mean day of low flow occurrence and the intensity of seasonality, or the seasonality  
histogram, which shows the occurrence of low flows in each month (Laaha and Blöschl, 2006). Colwell's predictability is  
another measure describing periodic signals (Colwell, 1974), mostly used in ecological studies. It consists of constancy (how  
70 natures describe (parts of) the seasonality of either climate or streamflow, yet none of them look at how climate seasonality  
translates into streamflow seasonality. As the transformation of climate input into streamflow is, after all, what we are trying to  
understand, investigating the seasonal aspect of that seems worthwhile. Relating streamflow to climate input also removes the  
arbitrariness of picking a start date (e.g. by defining a water year), which is a limitation of many signatures that relate flows to  
a date (e.g. the half flow date).

75 In this work, we propose the use of hydrological signatures based on how catchments attenuate the seasonal climate input  
(forcing). We approximate the input signal to a catchment (the forcing) by precipitation minus potential evapotranspiration and  
the output signal from a catchment by streamflow. We quantify the seasonal components of both signals by fitting sine waves to  
them, i.e. we extract their (annual) Fourier modes. As the period is fixed (one year), the incoming sine wave and the outgoing  
sine wave differ only in their amplitude, their phase and their mean. As the mean is rather a measure of the annual water  
80 balance, we are primarily interested in amplitude and phase. The differences in amplitude and phase are used as signatures  
describing the steady-state response of a catchment to periodic forcing. This idea is similar to the approach of Peters et al.  
(2003) who investigated drought propagation through groundwater using sinusoidal recharge, and to the approach of Obergfell  
et al. (2019) who used the seasonal behaviour as an additional signature in recharge estimation. The approach is also similar to  
approaches in transit time modelling (e.g. McGuire and McDonnell, 2006; Kirchner, 2016). Instead of focusing on the velocity  
85 of water particles, we, however, focus on the hydraulic response to periodic forcing, that is the celerity of the input "wave" of  
hydraulic potential (Harman, 2019). The proposed signatures are essentially also spectral domain signatures (Montanari and  
Toth, 2007), focusing only on a certain meaningful period – the annual period.

While there are other methods that quantify input-output relations, we propose the use of the seasonal signatures for several  
reasons. The seasonal signatures can be related to conceptual linear reservoirs (this will be outlined in Section 2), i.e. they can  
90 be interpreted in terms of simple conceptual model structures and parameter values (the reservoir time constants or response  
times). This gives them some hydrological interpretability (cf. discriminatory power; McMillan et al., 2017). Furthermore, by  
quantifying the delay between seasonal climate input and catchment output, we obtain a time scale that focuses on seasonal  
and thus rather slow dynamics. This might make it a valuable addition to methods focusing on event scales (e.g. recession  
analysis) and to other slow flow signatures such as the baseflow index (BFI), or the flow duration curve and parts thereof (e.g.

95  $Q_{95}$ ), which focus on volumes and frequencies, respectively. Lastly, the signatures do not require any parameters, they can be estimated directly from precipitation, potential evapotranspiration and streamflow data, which makes it straightforward to apply them to large samples of catchments.

In the following, we will first define the seasonal signatures, and we will present analytical solutions describing the response of linear reservoirs to periodic forcing (Section 2). Second, we will calculate the seasonal signatures for a range of catchments in the UK and in the US (Section 4, the data sources are presented in Section 3). We will explore how they relate to hydro-climatic forcing and catchment form, and we will interpret the underlying hydrological processes as well as limitations of the approach (Section 5). Finally, we will present an example application, in which we test whether two commonly used hydrological models (IHACRES, GR4J) can reproduce the observed ranges of seasonal signatures in the UK. This modelling experiment aims at exploring whether the signatures can be used as an additional source of information in model evaluation (Section 5.4).

## 2 Methods

### 2.1 Extracting seasonal components from time series

#### 2.1.1 Quantification of periodic components

To analyse the periodic components (Fourier modes) of time series we first need to quantify these components. While we could investigate the whole frequency spectrum of our time series and see how this is altered by a catchment (Montanari and Toth, 2007), we will focus on a period  $T$  of one year. The annual period has a clear physical meaning as it is the period the Earth moves in its orbit around the Sun, which is directly linked to the energy input to the Earth system. Furthermore, the annual mode is the strongest mode in the vast majority of catchments investigated here (see Supplement for further details). The input to a catchment, the forcing  $F$ , is approximated by precipitation  $P$  minus potential evapotranspiration  $E_p$  ( $F = P - E_p$ ). We use  $E_p$  to avoid the need for a model or additional data which would be needed to obtain actual evapotranspiration  $E_a$ . This might be particularly problematic in water-limited catchments, where actual evapotranspiration is much smaller than potential evapotranspiration, and in catchments where precipitation and potential evapotranspiration are out of phase. We will discuss that in Section 5. The seasonal component of the forcing  $F_{\sin}$  is given by (Milly, 1994):

$$F_{\sin} = \bar{F} \left( 1 + \delta_F \sin \left( \frac{2\pi}{T} t + \phi_F \right) \right) \quad (1)$$

where  $\bar{F}$  is the mean,  $\delta_F$  is the ratio between the amplitude and the mean (the dimensionless amplitude), and  $\phi_F$  is the phase (with respect to a reference date) of the seasonal forcing component. The output from a catchment is approximated by streamflow  $Q$ . The seasonal component of streamflow  $Q_{\sin}$  is given by:

$$Q_{\sin} = \bar{Q} \left( 1 + \delta_Q \sin \left( \frac{2\pi}{T} t + \phi_Q \right) \right) \quad (2)$$

where  $\bar{Q}$  is the mean,  $\delta_Q$  is the ratio between the amplitude and the mean, and  $\phi_Q$  is the phase (with respect to the same reference date) of the seasonal streamflow component.

Since we know the period  $T$  of interest, we need to quantify the mean, the amplitude and the phase of the periodic components. There are different methods to fit a sine curve of a certain period to data, i.e. to extract Fourier modes. We have compared two sine curve fitting, namely multiple linear regression and a method that makes use of the cross-covariance of two sine waves. Both methods lead to virtually the same results. A description and a comparison of the methods is shown in the Supplement. For the rest of the analysis, we will use results obtained by means of multiple linear regression (details on the fitting method can be found in the Supplement).

### 2.1.2 Calculation of seasonal signatures

Once we have extracted the seasonal components from our time series (precipitation minus potential evapotranspiration, streamflow), we can quantify how the outgoing sine wave  $Q_{\text{sin}}$  has been altered by the catchment by comparing it to the incoming sine wave  $F_{\text{sin}}$ . We define two metrics, the amplitude ratio and the phase shift, which together we call seasonal signatures. The amplitude ratio  $A$  is the ratio between the seasonal streamflow amplitude  $\delta_Q \bar{Q}$  and the seasonal forcing amplitude  $\delta_F \bar{F}$ :

$$A = \frac{\delta_Q \bar{Q}}{\delta_F \bar{F}} \quad (3)$$

Given a closed long-term water balance, the amplitude ratio should theoretically always be between zero and unity, that is, the streamflow amplitude cannot be larger than the forcing amplitude. The phase shift  $\phi$  is the difference between the phase of the seasonal streamflow component  $\phi_Q$  and the phase of the seasonal forcing component  $\phi_F$ :

$$\phi = \phi_Q - \phi_F \quad (4)$$

The phase shift should theoretically always be positive (the input should lead the output) and smaller than one year.

## 2.2 Linear reservoir theory

The derivations presented here all rely on the assumption of a linear time-invariant system (see e.g. Dooge, 1973, for an overview of linear theory of hydrologic systems). This implies that forcings of different wavelengths are not influencing each other. The assumption of linearity is invalid for most real systems, yet it is still widely made as it can yield useful insights.

A linear reservoir is described by:

$$Q = \frac{S}{\tau} \quad (5)$$

where  $Q$  [ $\text{mm d}^{-1}$ ] is the outflow from the reservoir,  $S$  is storage [mm] and  $\tau$  [d] is a time constant describing how fast (slow) the reservoir responds. Conservation of mass requires:

$$\frac{dS}{dt} = Q_{\text{in}} - Q \quad (6)$$

where  $Q_{\text{in}}$  is the inflow to the reservoir.

### 2.2.1 Periodic forcing of a linear reservoir

155 If we approximate the seasonal input to a linear reservoir by a sine wave of period  $T$  (e.g. one year), we can combine Equations (1), (5) and (6) to obtain:

$$\frac{dQ_{\sin}}{dt} = \frac{\bar{F}}{\tau} \left( 1 + \delta_F \sin \left( \frac{2\pi}{T}t + \phi_F \right) \right) - \frac{Q_{\sin}}{\tau} \quad (7)$$

We might neglect the (initial) phase if we choose a starting time  $t$  that is aligned with the seasonal forcing component ( $\phi_F = 0$ ). It can be shown that the steady state response of a linear reservoir to a sinusoidal input signal is a damped and phase shifted version of the input signal (see Supplement for a more detailed derivation; or Eriksson, 1971; Peters et al., 2003):

$$Q_{\sin}(t) = \bar{F} \left( 1 + \delta_F A \sin \left( \frac{2\pi}{T}t + \phi \right) \right) \quad (8)$$

where  $A$  is the amplitude ratio and  $\phi$  is the phase shift induced by a single linear reservoir.

$$A = \frac{1}{\sqrt{1 + (2\pi\frac{\tau}{T})^2}} \quad (9)$$

$$165 \quad \phi = \arccos \left( \frac{1}{\sqrt{1 + (2\pi\frac{\tau}{T})^2}} \right) = \arccos(A) \quad (10)$$

We can rewrite Equation (8) as follows:

$$Q(t) = \bar{Q} \left( 1 + \delta_Q \sin \left( \frac{2\pi}{T}t + \phi \right) \right) \quad (11)$$

In a mass conserving system in steady-state, the mean of the output should equal the mean of the input. If the means obtained from data are different, either the forcing term is inaccurate (e.g. due to differences between actual and potential evapotranspiration) or the streamflow term is inaccurate (e.g. due to other losses or gains). The product of input amplitude and amplitude ratio equals the output amplitude ( $\delta_F \bar{F} A = \delta_Q \bar{Q}$ ).

From Equations (9) and (10), we can see that the amplitude ratio and the phase shift are given by  $A$  and  $\arccos(A)$ , respectively. Since  $A$  is fully defined by the ratio between  $\tau$  and  $T$ , and  $T$  is usually known (e.g. one year), we can theoretically use  $A$  to determine the time constant  $\tau$  of the reservoir. This requires the identification of both the seasonal components of the input and output signal of that period (see Section 2.1), and assumes the system to behave as a single linear reservoir. Theoretically, we could also apply the theory to other periods than one year, but for the reasons stated above we only investigate the annual period.

The amplitude ratio  $A$  and the phase shift  $\arccos(A)$  can be plotted against each other for various values of  $\tau$  as shown in Figure 1. This results in a characteristic curve which captures the response of all single linear reservoirs. Different time constants  $\tau$  (as proportions of the period, here one year) lead to different positions on the curve. For very fast reservoirs, the phase shift is close to 0 days and the amplitude ratio is close to unity (that is, the signal is not attenuated at all). For very slow reservoirs, the signal is phase shifted up to 91 days and the amplitude ratio approaches 0. The maximum phase shift of about 91

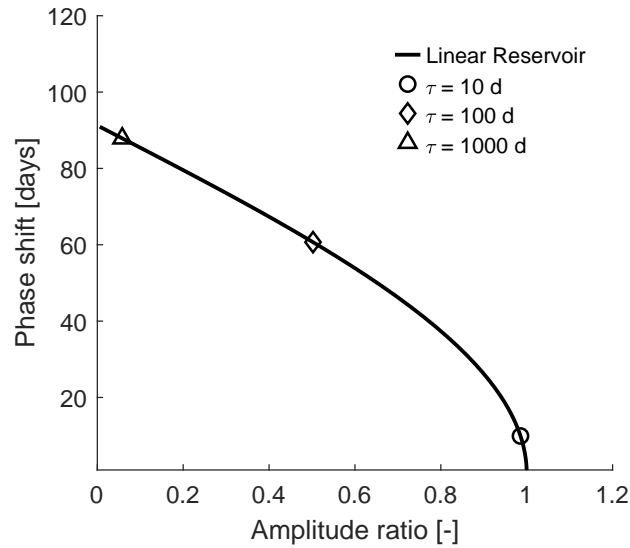


**Figure 1.** Amplitude ratio against phase shift for a single linear reservoir for varying time constants  $\tau$ . Three example time constants are indicated by the symbols.

days corresponds to a quarter of a period (90 degrees). Mathematically, this can be explained by Equation (10), as the arccosine of a quantity between 0 and unity (such as  $A$ ) ranges between 0 and 90 degrees.

185 Note the similarity of Figure 1 to Figure 3c in Kirchner (2016), which shows the relationship between phase shift and  
 amplitude ratio for gamma-distributed catchment transit time distributions. An exponential transit time distribution (a special  
 case of the gamma distribution) corresponds to a linear reservoir describing the velocity of particles. Similarly, a linear reservoir  
 describing the impulse response (the linear reservoir from Equation (5)), i.e. the celerity of the incoming wave of hydraulic  
 potential, corresponds to an exponential response time distribution or an exponential unit hydrograph (cf. Eriksson, 1971;  
 190 Dooge, 1973).

### 2.2.2 Combinations of linear reservoirs

Linear systems (Dooge, 1973) have the advantage that it is relatively straightforward to add more components, that is, reser-  
 voirs. It is quite common to have serial and/or parallel combinations in rainfall-runoff models. In theory, we can find analytical  
 solutions for the amplitude ratio and phase shift for all combinations of linear reservoirs (cf. to the transfer function approach  
 195 of Young, 1998, who identifies combinations of reservoirs that fit the data best in an inductive way). There are two basic  
 arrangements, a serial arrangement of reservoirs and a parallel arrangement of reservoirs.

### 2.2.3 Linear reservoirs in series

Linear reservoirs in series can be conceptualised as follows. Every outflow is the inflow to the next reservoir. Hence, if the  $i$ -th reservoir has a time constant  $\tau_i$ , the amplitude ratios  $A_i$  are multiplied and the phase shifts  $\phi_i$  are added (see Supplement for a more detailed derivation):

$$A_{\text{tot}} = \prod_{i=1}^n A_i \quad (12)$$

$$\phi_{\text{tot}} = \sum_{i=1}^n \phi_i = \sum_{i=1}^n \arccos(A_i) \quad (13)$$

Figure 2 shows the amplitude ratio plotted against the phase shift similar to Figure 1, but now with two linear reservoirs in series. The different lines are examples with fixed time constants of the first reservoir. They all start from the black line (from the points marked by the symbols in Figure 1), the characteristic curve for a single linear reservoir, which is the lower limit. Then, as the time constant of the second reservoirs increases, the lines "move" left and upwards, which corresponds to a decrease in amplitude ratio and an increase in phase shift. For example, the red line ( $\tau_1 = 10$  d) starts out with a phase shift of about 10 days, and ends at a phase shift of about 101 days, which is an increase of about 91 days, the maximum phase shift of the second reservoir. The lines cross each other as we allow  $\tau_2$  to be larger than  $\tau_1$ . This implies that sometimes a faster reservoir is followed by a slower one, and sometimes a slower reservoir is followed by a faster one. The grey shaded area contains all possible combinations for two reservoirs in series. The lower limit is a single linear reservoir. The upper limit corresponds to two reservoirs with the same time constant (a two-reservoir Nash cascade), which equals a gamma distribution with a shape parameter equal to 2 (Nash, 1957).

### 2.2.4 Linear reservoirs in parallel

Linear reservoirs in parallel result in a "mixture" of the outflows from each reservoir. The resulting flow is a combination of sine waves of the same period, weighted by the fraction  $p_i$  going into each reservoir. For the sake of simplicity, we only consider two reservoirs in parallel. We denote the fraction going into the second reservoir by  $p$ , and therefore the fraction going into the first reservoir by  $1 - p$ . Thinking of the second reservoir as the slow one,  $p$  might be compared to the idea of the baseflow index (BFI), the volumetric ratio between baseflow and total streamflow (Institute of Hydrology, 1980). For two reservoirs in parallel we get (see Supplement for a more detailed derivation):

$$A_{\text{tot}} = \sqrt{[(1-p)A_1 \cos \phi_1 + pA_2 \cos \phi_2]^2 + [(1-p)A_1 \sin \phi_1 + pA_2 \sin \phi_2]^2} \quad (14)$$

$$\phi_{\text{tot}} = \arctan \left( \frac{(1-p)A_1 \sin \phi_1 + pA_2 \sin \phi_2}{(1-p)A_1 \cos \phi_1 + pA_2 \cos \phi_2} \right) \quad (15)$$

Figure 3 shows the amplitude ratio plotted against the phase shift similar to Figure 1, but now with two linear reservoirs in parallel. We show multiple plots to highlight the three degrees of freedom: the two reservoir time constants and the fraction going into each reservoir. The latter is highlighted in Figure 3d, but also visible in Figures 3a-c. The grey shaded area contains



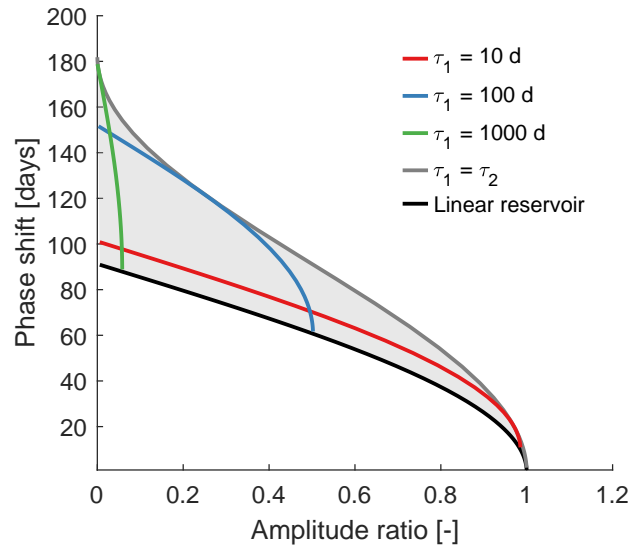


**Figure 2.** Amplitude ratio against phase shift for two linear reservoirs in series. Each line corresponds to a fixed time constant for the first reservoir ( $\tau_1$ ), while the time constant of the second reservoir varies ( $1 \text{ d} \leq \tau_2 \leq 10000 \text{ d}$ ; it is increasing from right to left). The black line indicates a single linear reservoir (the lower boundary). The grey line indicates the upper boundary where  $\tau_1 = \tau_2$ . The shaded area contains all possible combinations of amplitude ratio and phase shift for two linear reservoirs in series.

all the possible combinations for two reservoirs in parallel. The upper limit is a single linear reservoir. The lower limit is effectively given by the  $x$ - and the  $y$ -axis.

As an example, Figure 3a can be explained as follows:  $\tau_1$  is always 1 d, the fraction  $p$  going into the second reservoir is 0.3, and  $\tau_2$  starts with a value of 10 d and then increases. So at first, both reservoirs are rather fast and we get a high amplitude ratio and a small phase shift for the combined sine wave (see Equations (14) and (15)). Then, the second reservoir gets slower, leading to a decrease in amplitude ratio and an increase in phase shift. As the second reservoirs gets slower and slower, it will contribute less and less to the overall sine wave. For very high values of  $\tau_2$  (e.g. 10000 d), the sine wave coming out of the second reservoir is almost a straight line, so the combined sine wave is primarily consisting of the sine wave coming out of the first reservoir. Since only a fraction of  $1 - p = 0.7$  of the total input has gone into the first reservoir, the amplitude of the combined sine wave is approximately 0.7 times the input amplitude with a very small phase shift, as the first reservoir hardly attenuates the signal.

### 2.3 Seasonal signatures as a diagnostic tool for evaluating hydrological models

We use two conceptual rainfall-runoff models and we test whether the seasonal signatures can be used as a diagnostic tool to assess model performance (Gupta et al., 2008). In particular, we test whether the models are capable of reproducing the range of observed signatures without calibrating them to streamflow data (cf. Vogel and Sankarasubramanian, 2003). This

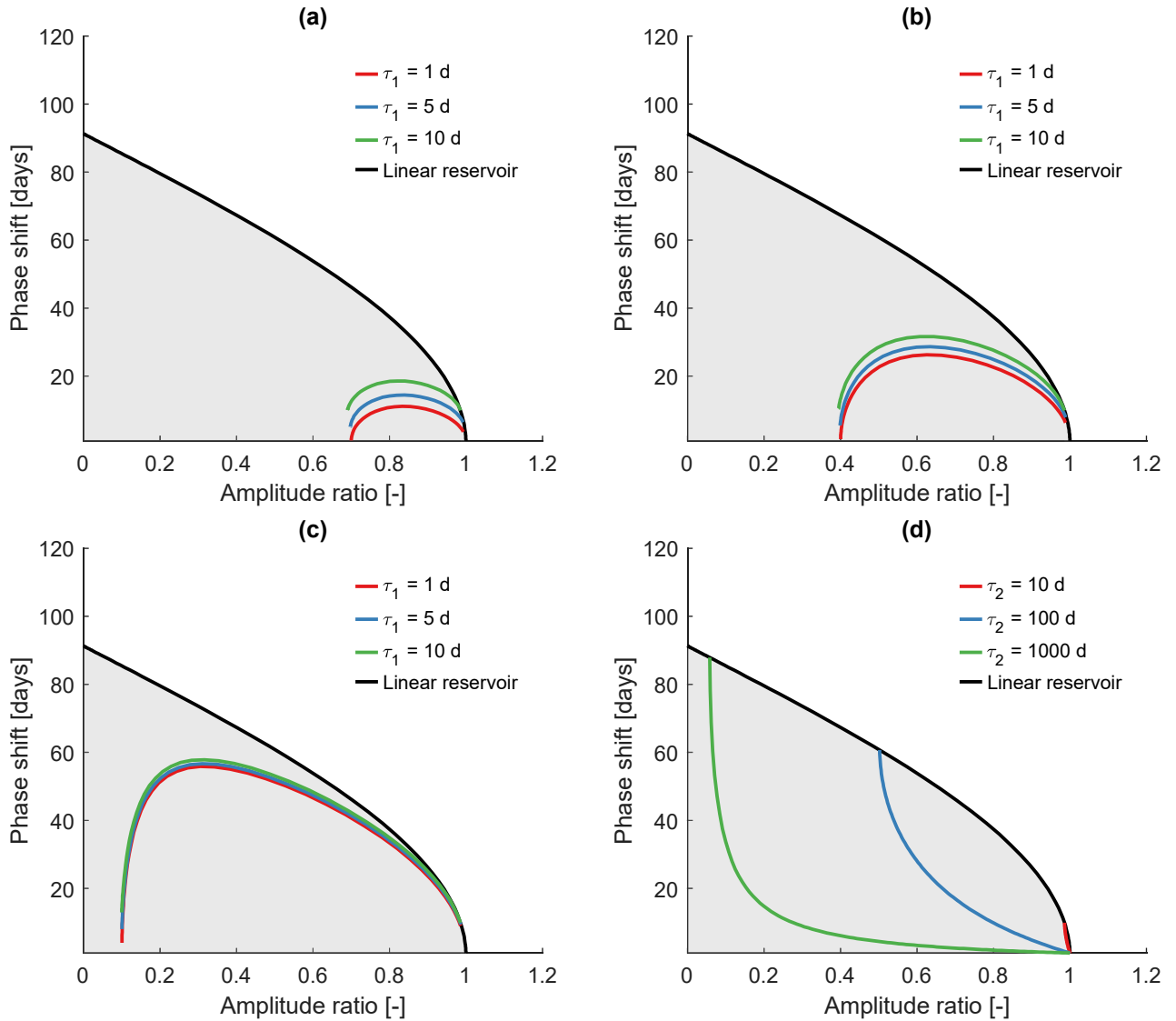


**Figure 3.** Amplitude ratio against phase shift for two linear reservoirs in parallel. **(a)** Each line has a fixed time constant for the first reservoir ( $\tau_1$ ), while the time constant of the second reservoir varies ( $10 \text{ d} \leq \tau_2 \leq 10000 \text{ d}$ ; it is increasing from right to left). The fraction  $p$  going into the second reservoir is 0.3. **(b)** Same as **(a)** with  $p = 0.6$ . **(c)** Same as **(a)** with  $p = 0.9$ . **(d)** Each line has a fixed time constant for the first reservoir ( $\tau_1 = 1$  d), and for the second reservoir ( $\tau_2$ ). The fraction  $p$  going into the second reservoir is varied (it is increasing from right to left). The shaded area contains all the possible combinations of amplitude ratio and phase shift for two linear reservoirs in parallel.

modelling experiment is intended to test whether the proposed signatures have the potential to be a useful additional source of information in model building and evaluation. We do not intend (or suggest) that the presented evaluation approach can replace existing model evaluation methods. We limit the analysis to two models and 40 catchments to keep the computational demand manageable. We also limit the model evaluation to catchments in the UK, as the seasonal signatures are unreliable in arid catchments (see Section 5). The subset of catchments is described in Section 3 and in the Supplement.

The first model is the IHACRES model. It is conceptually relatively similar to the considerations in Section 2. It has a soil moisture store (non-linear deficit store), and two parallel linear stores for fast flow and for slow flow (Croke and Jakeman, 2004). It has been used in many modelling studies in Australia (Post and Jakeman, 1999) and also in the UK (Sefton and Howarth, 1998). The second model is the GR4J model. It also has a parallel flow structure, but the internal parametrisation is different. It contains more non-linearities and it has fixed internal parameters. Additionally, it has a groundwater exchange parameter aimed at representing inter-catchment groundwater flows. It has been used in many modelling studies in France (Perrin et al., 2003), in the UK (Smith et al., 2019; Harrigan et al., 2018b) and in the US (Oudin et al., 2018). We use the implementations of the two models in the MARRMoT toolbox v1.2 (Knoben et al., 2019a), a Matlab toolbox containing many hydrological models aimed at model comparison studies. The pure delay function in the MARRMoT implementation of IHACRES is set to 0, making it (conceptually, not necessarily numerically) equal to the version used by Croke and Jakeman (2004). In our modelling experiment, IHACRES has therefore 6 parameters, and GR4J has 4 parameters. Detailed information on the parameter ranges and on model warm-up periods can be found in the Supplement.

To test which ranges of seasonal signatures the two models can reproduce, we run a Monte-Carlo sampling experiment. We sample parameter sets for both models using Latin Hypercube sampling, an efficient sampling method (Cheng and Druzzdel, 2000) that assumes uniform prior parameter distributions. With the parameter sets obtained, we run both models for each of the 40 catchments, i.e. we use the same parameter sets for each catchment. To test for robustness, we sample an increasing number of parameter sets (20000 parameter sets are considered sufficient, see Supplement for more information). We then use the modelled streamflow time series to calculate three hydrological signatures per parameter set: the two seasonal signatures presented here and the baseflow index (BFI). The resulting modelled signatures are compared to observed signatures and explored in a rather general way, as we want to examine what the models can do without actually calibrating them to streamflow data (cf. Vogel and Sankarasubramanian, 2003). That is, we are not interested in finding the "best" parameter set, but in whether a certain model (given certain parameter ranges) is generally capable of reproducing the signatures we observe.

### **3 Data**

#### **3.1 Data sources**

We use catchment data from Great Britain and the United States. The data for the UK are obtained from different sources. Daily streamflow data, catchment characteristics and catchment boundaries are obtained from the NRFA (National River Flow Archive, 2019), precipitation data from CEH-GEAR (Tanguy et al., 2016), and potential evapotranspiration data from CHES-PE (Robinson et al., 2016). For the model evaluation we select catchments that are part of the UK Benchmark Network

**Table 1.** Hydrological signatures and catchment attributes used in this study.

Name	Description	Unit	Range	Reference
Hydrological signatures				
BFI	Baseflow index	[-]	[0, 1]	Institute of Hydrology (1980)
$A$	Amplitude ratio	[-]	[0, 1] <sup>1</sup>	Equation (3)
$\phi$	Phase shift	[d]	[0, 365] <sup>2</sup>	Equation (4)
Catchment attributes				
$I_m$	Moisture index	[-]	[-1, 1]	Knoben et al. (2018)
$I_{m,r}$	Moisture index seasonality	[-]	[0, 2]	Knoben et al. (2018)
$f_s$	Snow fraction	[-]	[0, 1]	Knoben et al. (2018)
PROPWET	Catchment wetness index	[-]	[0, 1]	National River Flow Archive (2019)
% fractured aquifer	Fraction of highly productive fractured aquifer	[%]	[0, 100]	National River Flow Archive (2019)
% carbonate rock	Fraction of carbonate sedimentary rock	[%]	[0, 100]	Addor et al. (2017)

<sup>1</sup>Should in theory be smaller than unity. <sup>2</sup>Should theoretically always be positive and in practice be smaller than one year. Further discussions on the possible ranges of the seasonal signatures can be found in the text.

(Harrigan et al., 2018a), which describes catchments in the UK that are near-natural. The subset of catchments is chosen to be  
 275 representative of the UK, details are shown in the Supplement. The data for the US are obtained from the CAMELS dataset  
 (Newman et al., 2015; Addor et al., 2017). CAMELS includes daily precipitation, potential evapotranspiration (we use Daymet  
 forcing data) and streamflow data as well as a wide range of catchment attributes for 671 catchments in the contiguous US.  
 We trim the daily data to contain only full water years (starting 1 October) and we analyse data from 1989 to 2009. We also  
 remove catchments with missing records during that time period. While we need to pick a start date for the analysis, this date  
 280 does not influence the results (e.g. using 1 January as starting date would result in the same phase shift).

### 3.2 Hydrological signatures and catchment attributes

We calculate different hydrological signatures and we use different catchment attributes, all summarised in Table 1. The climate  
 indices from Knoben et al. (2018) are based on monthly averages and they need to be interpreted as follows. A moisture index  
 $I_m$  of 1 indicates the most humid (energy-limited) catchments, a moisture index of -1 indicates the most arid (water-limited)  
 285 catchments. A moisture index seasonality  $I_{m,r}$  of 0 indicates catchments where the climate stays constant throughout the year,  
 a moisture index seasonality of 2 indicates catchments where the climate switches between fully arid and fully humid within  
 the year.

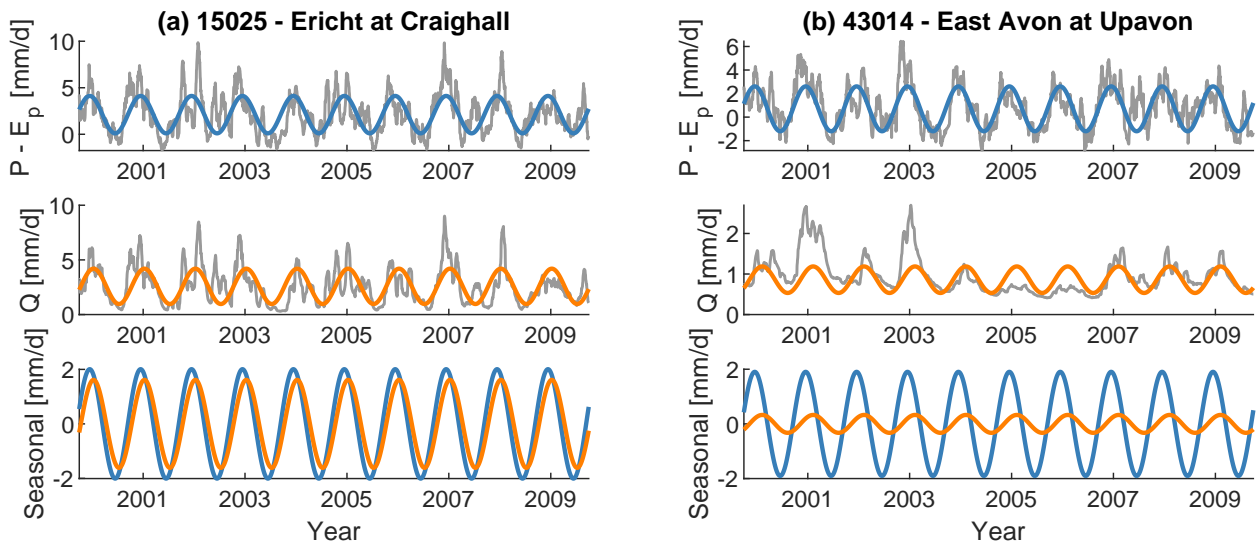


**Figure 4.** Climate input ( $P - E_p$ ; blue) and catchment output ( $Q$ ; orange) for two example catchments in the UK, and their respective seasonal components. The time series are smoothed using a 30-day moving mean. The Ericht is a rather responsive catchment (BFI = 0.47), while the East Avon has a large baseflow component (BFI = 0.89). Note that for the bottom plots ("Seasonal") the mean values of the sine curves are set to zero.

## 4 Results

### 4.1 Extracting seasonal components from time series

290 First, we extract seasonal components from  $P - E_p$  (forcing) and  $Q$  (streamflow) for all catchments. The resulting sine wave  
 parameters are then used to calculate the amplitude ratios (Equation (3)) and phase shifts (Equation (4)), respectively. Figure  
 4 shows  $P - E_p$  and  $Q$  for two catchments alongside their seasonal (sinusoidal) components. Both catchments experience  
 a similar forcing, but their response is very different. The Ericht at Craighall, a rather responsive catchment, shows a sea-  
 295 sonal streamflow component that is very similar to the seasonal forcing component. In contrast, the East Avon at Upavon, a  
 groundwater-dominated catchment, shows a strongly attenuated seasonal streamflow component. For our seasonal signatures  
 this would mean (a) that the responsive catchment has a high amplitude ratio, i.e. the streamflow amplitude is almost as large  
 as the forcing amplitude, while the groundwater-dominated catchment has a low amplitude ratio. And (b) that the respon-  
 sive catchment has a small phase shift, i.e. it responds quickly to the (seasonal) forcing, while the groundwater-dominated  
 catchment has a large phase shift.

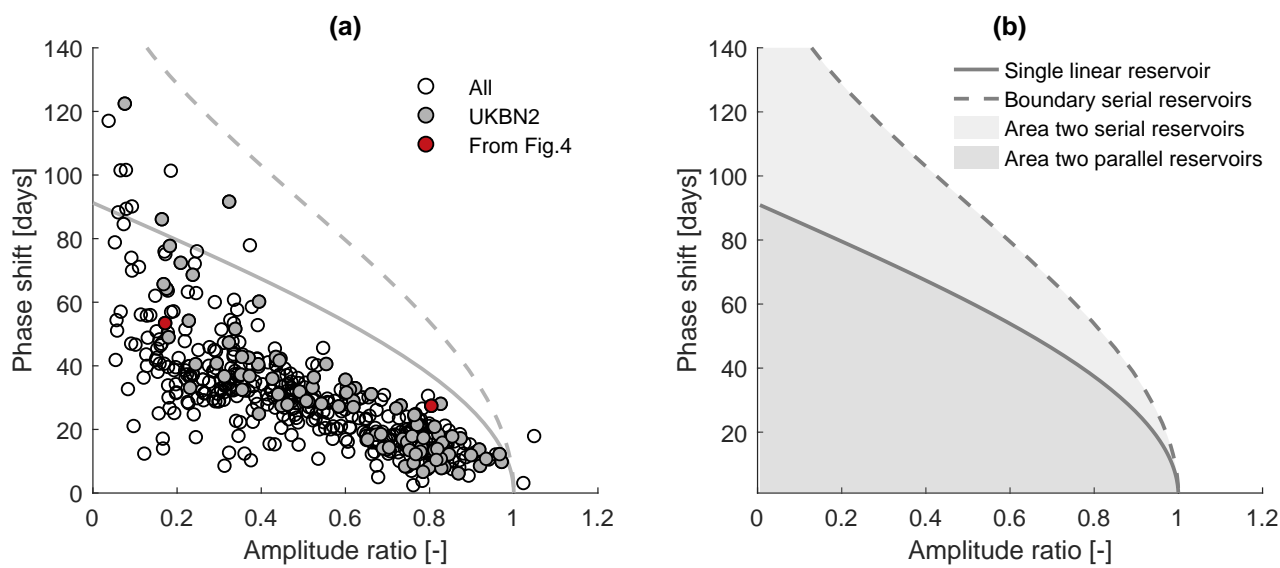


**Figure 5.** (a) Amplitude ratio against phase shift for UK catchments. Grey dots indicate benchmark catchments, red dots indicate the two catchments shown in Figure 4. Grey solid line indicates a single linear reservoir, grey dashed line indicates the outer envelope for two reservoirs in parallel. Note that both axes are limited (two catchments are not shown). (b) Theoretical areas and limits for single linear reservoir, two reservoirs in series, and two reservoirs in parallel.

## 300 4.2 Seasonal signatures of observed catchment data

To visualise the seasonal signatures, we plot the amplitude ratios and phase shifts in a similar way as in Figures 1, 2, and 3. This is shown in Figure 5a for all UK catchments. These include catchments with human influences, such as groundwater abstractions, man-made reservoirs or water transfers. The overall pattern in Figure 5a is very similar to the pattern using benchmark catchments alone (grey dots). We therefore use all of the catchments, noting that a few catchments might be  
 305 unsuitable for individual analyses.

Figure 5a shows that most of the catchments fall below the solid grey line, the line which indicates the type of response that could be simulated by a single linear reservoir (see Figure 5b). The area below the solid line can be simulated by two reservoirs in parallel. This would be the most parsimonious way to reproduce the observed behaviour if we decide to construct our model using linear reservoirs only. A few catchments plot above the solid line. For these catchments, the most parsimonious way to  
 310 reproduce the pair of observed amplitude ratio and phase shift would therefore be two reservoirs in series. Very few catchments have an amplitude ratio larger than unity. While this could be caused by various errors in the data, it is likely due to erroneous catchment areas and/or the presence of inter-catchment groundwater flows or water transfers. If a catchment receives more net rainfall than the surface catchment area suggests (runoff ratio > 1), the amplitude in the output signal (streamflow) can be larger than the amplitude in the (erroneous) input signal.

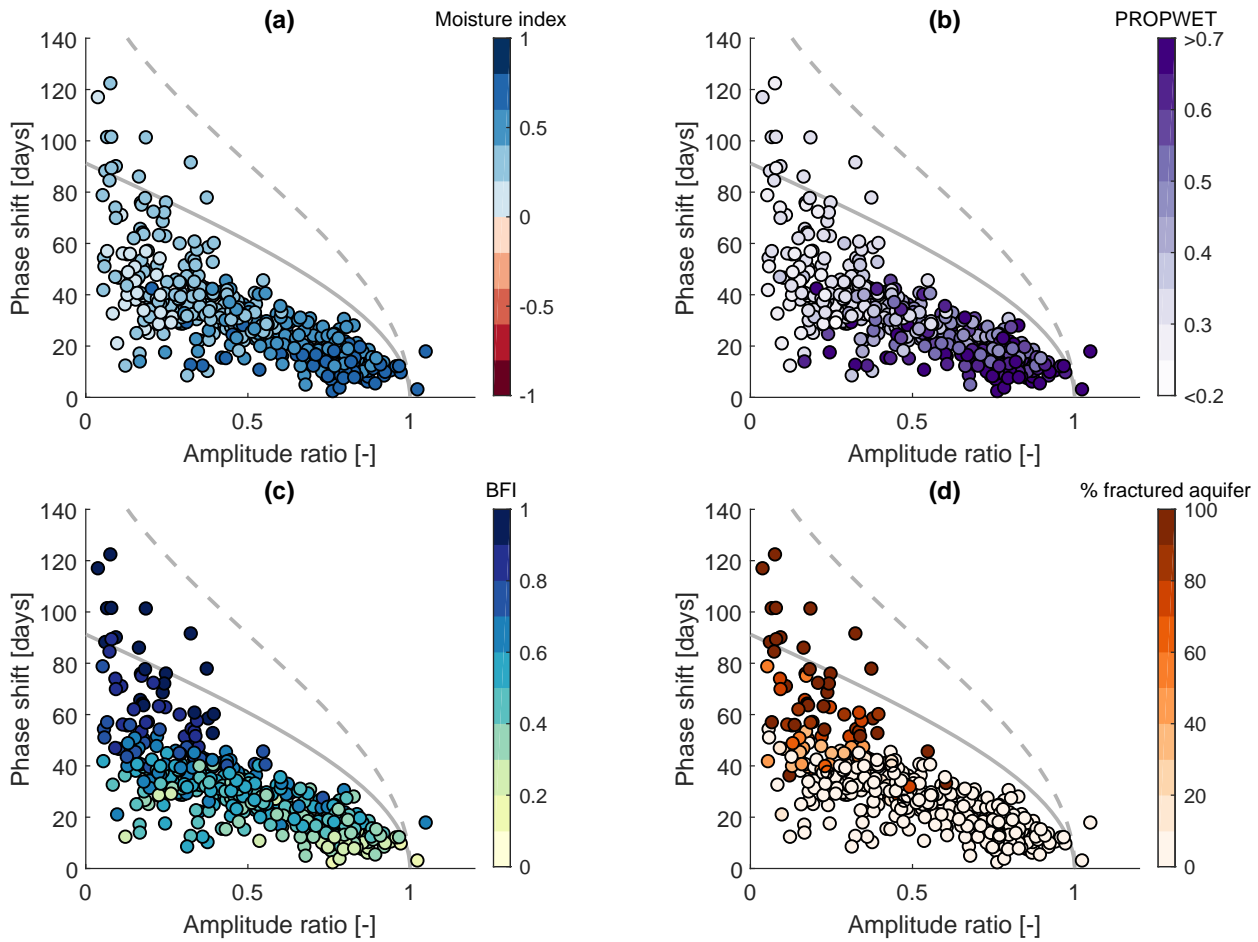


**Figure 6.** Amplitude ratio against phase shift for UK catchments. Grey solid line indicates a single linear reservoir, grey dashed line indicates the outer envelope for two reservoirs in parallel. Colours indicate (a) the moisture index, (b) the catchment wetness index, (c) the baseflow index, and (d) the fraction of highly productive fractured aquifer. Note that both axes are limited (two catchments are not shown).

### 315 4.3 Relationship between seasonal signatures and catchment attributes – UK

Figure 6 shows pairs of amplitude ratios and phase shifts, coloured according to different hydrological signatures and catchment attributes, respectively (explained in Table 1). Corresponding correlation coefficients can be found in Table 2. Figure 6a shows a clear pattern between the moisture index and the seasonal signatures. Generally, the less humid the catchments, the lower the amplitude ratio and the larger the phase shift. In other words, drier catchments attenuate the incoming forcing signal more strongly. This might partly be because we use potential evapotranspiration as our forcing. Lower actual evapotranspiration than potential evapotranspiration leads to a decreased input amplitude and thus to a higher amplitude ratio. Most of the very

320

**Table 2.** Pearson and Spearman correlation coefficients between seasonal signatures and catchment attributes for UK catchments.

Pearson	Amplitude ratio	Phase shift	$I_m$	PROPWET	BFI	% fractured aquifer
Amplitude ratio	1.00	-0.60	0.80	0.74	-0.58	-0.49
Phase shift	-0.60	1.00	-0.49	-0.50	0.66	0.58
Spearman	Amplitude ratio	Phase shift	$I_m$	PROPWET	BFI	% fractured aquifer
Amplitude ratio	1.00	-0.80	0.82	0.78	-0.58	-0.51
Phase shift	-0.80	1.00	-0.76	-0.75	0.77	0.60

**Table 3.** Pearson and Spearman correlation coefficients between seasonal signatures and catchment attributes for CAMELS catchments.

Pearson	Amplitude ratio	Phase shift	$I_m$	$I_{m,r}$	BFI	% carbonate rock
Amplitude ratio	1.00	-0.26	0.75	0.31	0.06	-0.16
Phase shift	-0.26	1.00	-0.39	-0.51	-0.14	0.26
Spearman	Amplitude ratio	Phase shift	$I_m$	$I_{m,r}$	BFI	% carbonate rock
Amplitude ratio	1.00	-0.46	0.78	0.23	0.04	-0.15
Phase shift	-0.46	1.00	-0.32	-0.64	0.06	0.36

humid catchments plot close together and the relationship between amplitude ratio and phase shift seems to be almost linear. Less humid catchments (note that in the UK none of the catchments are actually water-limited at the annual scale) show a larger spread, especially regarding the phase shift. Figure 6b shows a very similar pattern between the catchment wetness index and the seasonal signatures. Wetter catchments exhibit higher amplitude ratios and lower phase shifts, and vice versa. The catchment wetness index is strongly correlated with the moisture index (Spearman rank correlation of 0.94). Figure 6c shows a clear pattern between the baseflow index and the seasonal signatures. In contrast to the moisture index, where the stratification follows mostly the  $x$ -axis (amplitude ratio), the stratification follows mostly the  $y$ -axis (phase shift). Catchments with high BFIs exhibit low amplitude ratios and large phase shifts, and vice versa. Finally, in Figure 6d we can see that catchments underlain by highly productive fractured aquifers exhibit (with a few exceptions) low amplitude ratios and large phase shifts.

#### 4.4 Relationship between seasonal signatures and catchment attributes – US

Figure 7 shows pairs of amplitude ratios and phase shifts for the US, coloured according to different hydrological signatures and catchment attributes, respectively (explained in Table 1). Corresponding correlation coefficients can be found in Table 3. Catchments with significant snow fraction ( $f_s > 0.001$ ) are removed, as snow presents another hydrological process which is not the focus of this study. Generally, snow adds another storage process, and this is reflected in large phase shifts observed in snowy catchments (see Supplement for more information). The non-snowy catchments in the US show a similar trend to the catchments in the UK. Yet generally, the amplitude ratios are lower and the phase shifts larger compared to the UK (note that the  $y$ -axes in Figure 7 differ in their range from the  $y$ -axes in Figure 6). Humid catchments tend to have higher amplitude ratios and smaller phase shifts (Figure 7a). Climate seasonality, indicated by the moisture index seasonality (see Figure 7b), also



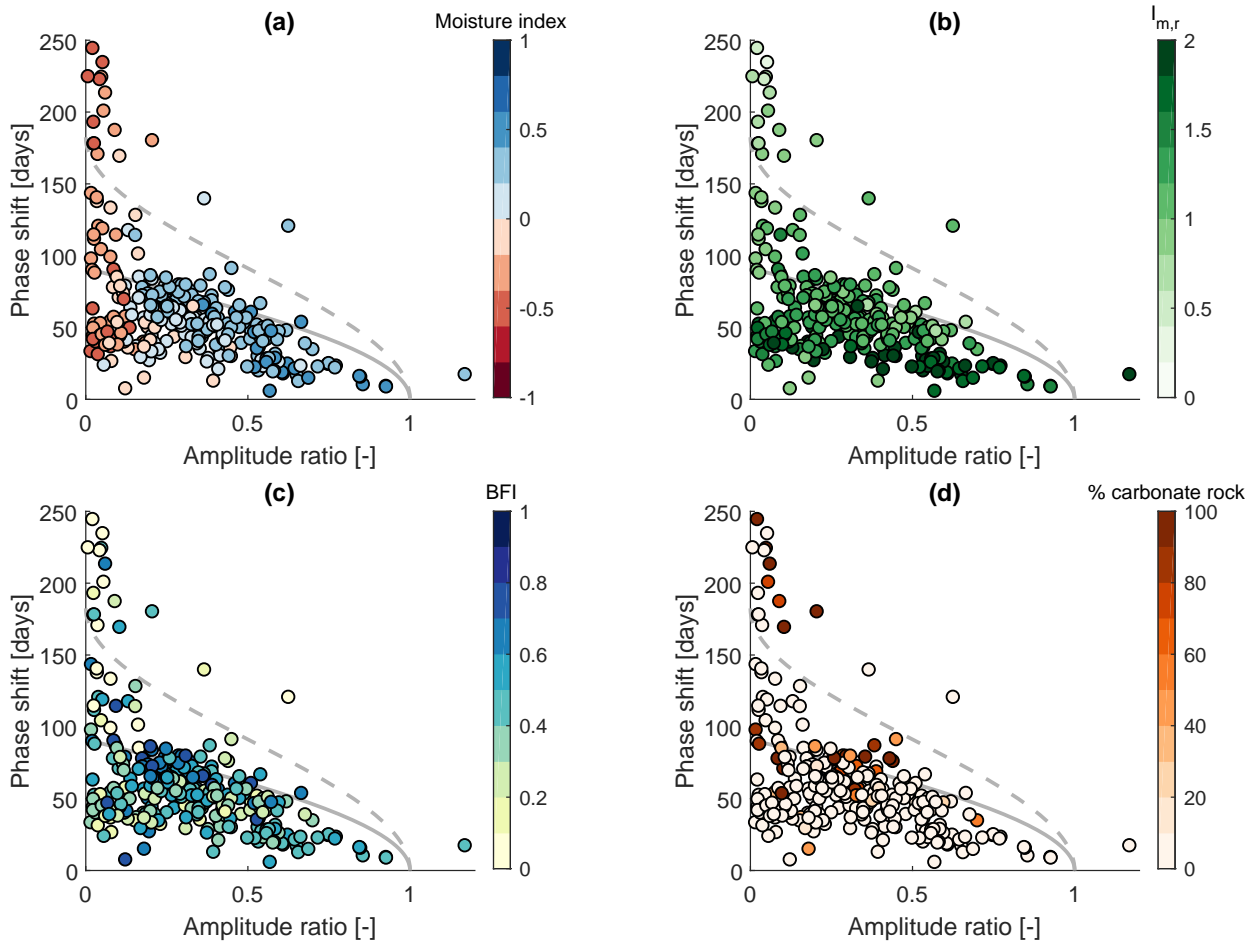


**Figure 7.** Amplitude ratio against phase shift for CAMELS catchments. Catchments with snow fraction ( $f_s > 0.001$ ) are removed from the analysis. Grey solid line indicates a single linear reservoir, grey dashed line indicates the outer envelope for two reservoirs in parallel. Colours indicate (a) the moisture index, (b) the moisture index seasonality, (c) the baseflow index, and (d) the fraction of carbonate sedimentary rock. Note that both axes are limited (12 catchments are not shown) and that the range of the phase shift-axis is different from Figure 6.

340 influences the seasonal signatures. Catchments with a larger moisture index seasonality, i.e. a more variable monthly moisture  
 index over the year, tend to have smaller phase shifts. The BFI (Figure 7c) does not show such a clear pattern as for the UK  
 catchments (Figure 6c). Similarly, subsurface properties such as the fraction of carbonate sedimentary rock (Figure 7d; and  
 other attributes not shown here) only show a weak relationship with the seasonal signatures. Catchments with larger fractions  
 of carbonate sedimentary rocks tend to have lower amplitude ratios and larger phase shifts. The overall pattern, however, is  
 345 rather scattered. Contrary to the UK, some of the catchments in the US plot outside the area that can be modelled by either two  
 reservoirs in series or in parallel and some catchments have phase shifts larger than 182 days, the approximate limit for two

reservoirs in series. These catchments are very arid and the low moisture seasonality index indicates that most the precipitation in these catchments falls when potential evapotranspiration is highest, i.e. in summer.

#### 4.5 Seasonal signatures as a diagnostic tool for evaluating hydrological models

350 In a similar fashion as for the observed catchment data, we now investigate the model runs using IHACRES and GR4J. Figure 8 shows the resulting amplitude ratios and phase shifts for all model runs, that is for 20000 parameter sets using data from a subset of 40 catchments in the UK. These plots show which combinations of seasonal signatures (and BFI) can be obtained with each model, given the forcing of 40 different catchments covering most of the hydro-climatic variability of the UK, and given the parameter ranges chosen. They hence show the "signature space" of a model in the dimensions given by amplitude ratio and phase shift (and BFI).  
355

IHACRES (Figure 8a) shows a pattern that covers the area that can be modelled by two reservoirs in parallel, and a large fraction of the area that can be modelled by two reservoirs in series (see Figures 2 and 3). The BFI spans the whole range from 0 to 1. IHACRES can reproduce the observed amplitude ratios and phase shifts, although one catchment sits just at the boundary of the point cloud. GR4J (Figure 8b) covers a different signature space. The phase shift never exceeds 110 days, the  
360 amplitude ratio often exceeds unity, and the BFI tends to be high. GR4J can reproduce most of the observed amplitude ratios and phase shifts, except for catchments with very large phase shifts. Furthermore, it struggles to simultaneously reproduce the observed phase shifts and BFIs.

Both models sometimes yield phase shifts that are close to one year (not shown here), which are effectively negative phase shifts. Negative implies that the periodic component of  $Q$  leads the periodic component of  $P - E_p$ . This can happen if actual  
365 evapotranspiration  $E_a$  differs considerably from potential evapotranspiration  $E_p$ , and hence most of the input seasonality stems from  $P$  (and not  $E_p$ ). This can be observed in a few catchments in the US (not shown here). It is only observed once in the UK (in a catchment with a man-made reservoir, not shown here), and therefore we do not investigate these model runs further.

Figure 9 shows distributions ("one-dimensional signatures spaces") for three hydrological signatures for the 40 catchments investigated here. These plots tell us which signature values a model tends to produce (given a certain sampling scheme),  
370 the ranges of signatures a model can reproduce (given the parameter ranges chosen), and how (much) a signature varies with varying forcing.

Figure 9 displays similar information as Figure 8, yet without considering interactions between the three signatures. IHACRES can produce amplitude ratios from 0 to 1 and phase shifts up to 182 days (which is the limit for two reservoirs in series) and larger. GR4J can produce amplitude ratios that clearly exceed one, and cannot model phase shifts larger than 110 days (given  
375 the parameter ranges chosen). For both models, more arid forcing leads to lower amplitude ratios and larger phase shifts, and vice versa. For the BFI (Figures 9c,f) we can see that IHACRES covers the whole possible space (0 to 1) relatively evenly. GR4J tends to produce very high BFIs for almost every parameter set. BFIs smaller than 0.5 are possible with GR4J, but rather rare (or unlikely).

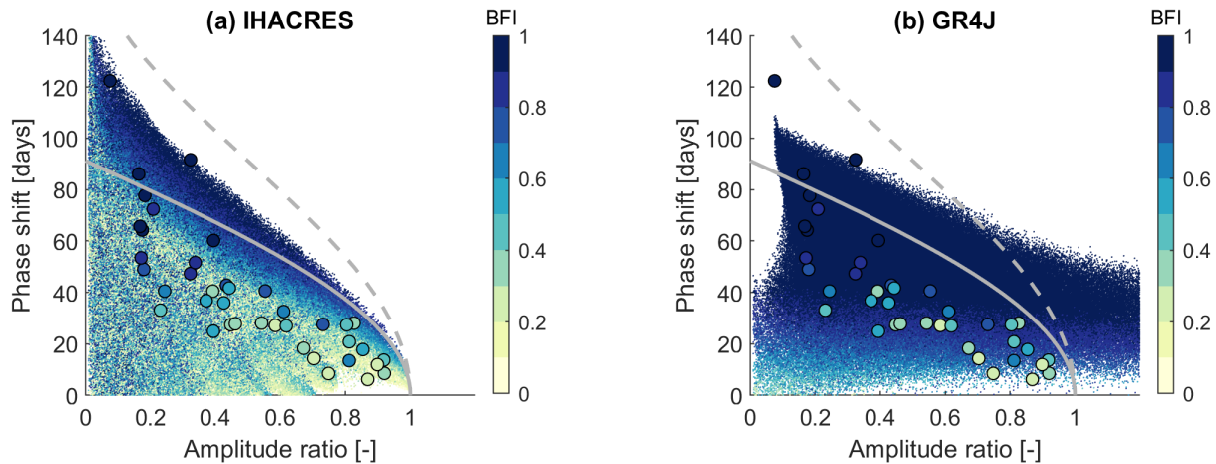


**Figure 8.** Amplitude ratio against phase shift for 40 catchments in the UK using 20000 parameter sets each for **(a)** IHACRES and **(b)** GR4J. The large dots show the observed signatures of the 40 catchments used for the modelling experiment. Colours indicate the BFI. Note that both axes are limited.

## 5 Discussion

### 380 5.1 Representation of seasonal components by sine waves and limitations of the approach

A sine wave is a simple way of describing the seasonality of a signal. The results suggest that for most of the catchments investigated here, this approach is reasonable and efficient. Figure 4 shows that the average seasonal pattern is captured by the fitted sine waves. Differences between years cannot be captured by our approach, as we fit a single sine wave to describe the average seasonal behaviour. To robustly capture the average seasonal behaviour, we need relatively long time series. Comparing  
 385 results from two different 10 year periods shows that the signatures are robust for the majority of catchments, i.e. their values do not differ substantially from one time period to the other (details are shown in the Supplement).

The UK catchments and most of the US catchments exhibit a relatively strong unimodal (climate) seasonality (see e.g. Knoben et al., 2018). In other climates with a less distinct seasonal pattern, or with two seasons per year (Knoben et al., 2019b), our approach will not work. Semi-arid and arid catchments also tend to have a less smooth seasonal input, as water  
 390 availability is more fragmented (Peters et al., 2003). Water-limited catchments can show a strong difference between potential evapotranspiration and actual evapotranspiration, which limits the applicability of our approach (we will discuss that later in more detail). We exclude catchments where precipitation is falling as snow. While snowy catchments are typically also strongly seasonal (Schaeffli, 2016), this seasonality is mostly a climate phenomenon. It is rather related to temperature seasonality and not to the response of a catchment to periodic forcing.

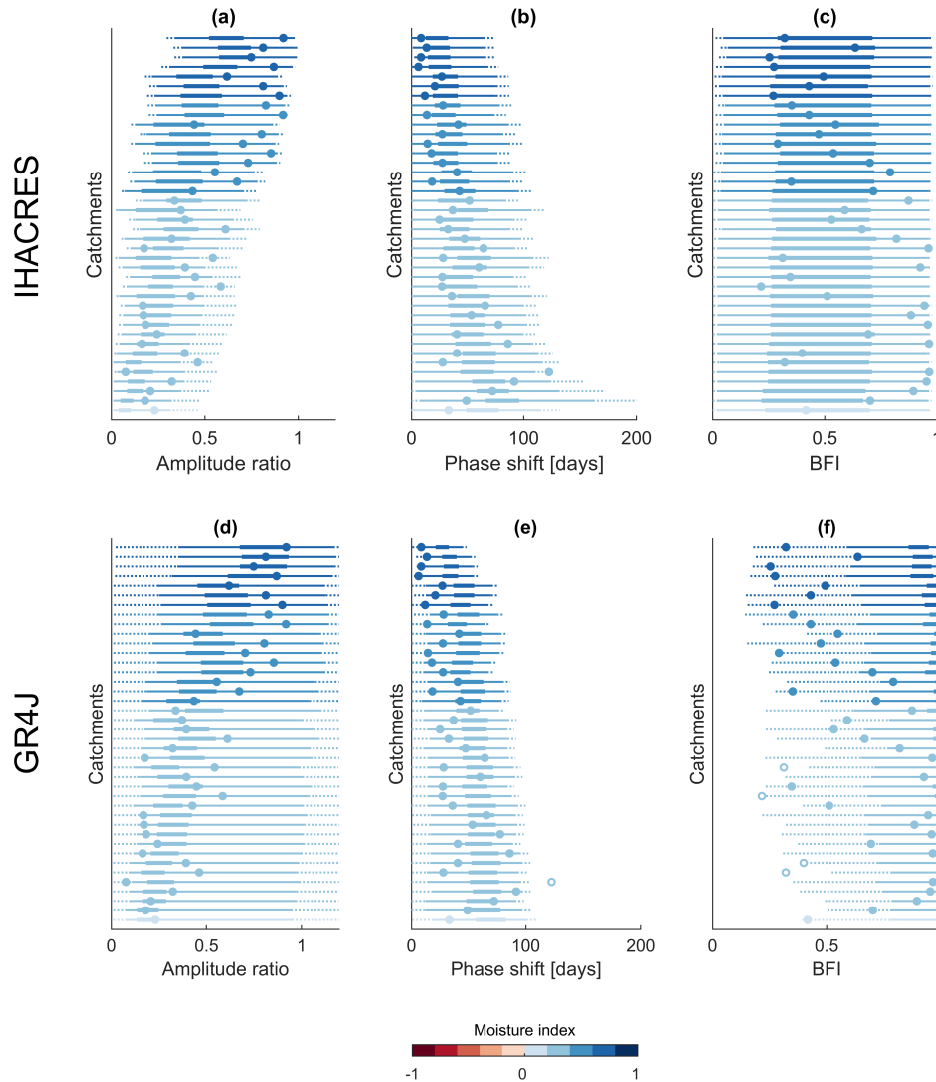


**Figure 9.** Distributions of different hydrological signatures resulting from the modelling experiment. Each line stands for one of the 40 catchments and the colours indicate the corresponding moisture index. The distributions of the modelled signatures are indicated by box-whisker-type plots. The thick line spans from the 25th to the 75th percentile. The thin line spans from the 1st (75th) to the 25th (99th) percentile. The dotted line indicates values below (above) the 1st (99th) percentile. The circles indicate the observed signature values, while filled circles indicate that the observed signature is inside the modelled signature space and vice versa. (a), (b), and (c) show results for IHACRES. (d), (e), and (f) show results for GR4J. Model runs with amplitude ratios lower than 0.01, amplitude ratios larger than 1.2, or phase shifts larger than 200 days have been removed.

The results, in particular Figures 5 and 6 and Table 2, show clear patterns in the seasonal signatures. We can see that the seasonal response in the UK can be simulated by either two reservoirs in series or two reservoirs in parallel. This does not mean that there are no other configurations of more reservoirs leading to the same pairs of amplitude ratio and phase shift. Rather, two reservoirs in series and in parallel, respectively, are the most parsimonious reservoir configuration to reproduce the observed seasonal behaviour. Of course, two reservoirs in parallel and two reservoirs in series, respectively, might be seen as "special cases" of a soil reservoir followed by a fast and a slow reservoir, i.e. a three-reservoir arrangement. Furthermore, there might be concepts other than reservoirs which can explain the observed behaviour. Still, the observed patterns, both where the catchments plot in the amplitude ratio vs. phase shift plot (Figure 5) and how the catchment attributes relate to that (Figure 6), suggest that the seasonal signatures are indeed a window into catchment functioning (Berghuijs et al., 2014) and thus have discriminatory power (McMillan et al., 2017; Addor et al., 2018).

Figures 6a and 6b show how climate aridity and catchment wetness influence amplitude ratio and phase shift. The observation that more humid catchments respond more quickly to forcing (Figures 6a and 6b) concurs with our understanding of these catchments. Wetter and therefore more saturated catchments partition the incoming water mostly into fast flow. The hydrograph closely resembles the forcing, which can also be seen in Figure 4 for the responsive Ercht river. The drier the catchments become, the more water is able to infiltrate and subsurface properties become more important. This might explain why the spread becomes larger for less humid and hence less saturated catchments. In less humid catchments, actual evapotranspiration is more likely to deviate from potential evapotranspiration. This might be another reason for the greater attenuation in drier catchments, as the actual input ( $P - E_a$ ) is lower than the theoretical one we compare to ( $P - E_p$ ). In the UK the assumption that  $E_a = E_p$  seems reasonable (see Supplement for further information). In more arid regions, such as parts of the US (see Section 5.3), this assumption is invalid.

The variability among UK catchments that cannot be explained by catchment wetness can mostly be explained by subsurface properties and the associated response time of a catchment. Catchments with high BFIs and thus large baseflow components show lower amplitude ratios and larger phase shifts, that is a more damped and lagged response (Peters et al., 2003). This can also be seen in Figure 4 for the groundwater-dominated East Avon river. The relationship between BFI and the seasonal signatures (Figure 6c) is not surprising, yet since the relationship is not unique, the seasonal signatures add another piece of information. In particular, the phase shift adds a time scale, which quantifies how long – on average – the seasonal input is delayed to become the seasonal output. While the phase shift is only a few days for the most responsive catchments, in the slowest catchments the seasonal signal is shifted up to four months. Since the BFI is rather a consequence of a catchment's hydrological behaviour (as are the seasonal signatures) than an attribute of a catchment, the BFI cannot be seen as a cause for the observed patterns in the seasonal signatures. It cannot be used, for example, as a predictor in ungauged catchments. A qualitative attribute that could theoretically be available in ungauged catchments, the fraction of highly productive fractured aquifer, reinforces the influence of the subsurface (Figure 6d). Except for a few catchments, catchments underlain by such an aquifer exhibit very large phase shifts. In fact, all the catchments above the single reservoir line are underlain by highly

productive aquifers. In these catchments, mostly underlain by Chalk, almost all the incoming water infiltrates into the aquifer, and the fast flow component often is negligible. This might explain why they do not behave like reservoirs in parallel, but rather like reservoirs in series, e.g. a soil reservoir (recharge) and a very slow groundwater reservoir. The few catchments which are underlain by highly productive aquifers, but do not exhibit large phase shifts, are typically overlain by rather impermeable drift, which stops water from infiltrating into the aquifer below.

Many models frequently used (and some of them developed) in the UK have a parallel flow structure, and catchments are usually conceptualised as having a fast and a slow component. While parametrisations and model structures vary between models, an overall parallel flow structure following a soil moisture module can be found in the PDM model (Moore, 2007), the TOPMODEL modelling concept (consisting of two fast flow responses; Beven and Kirkby, 1979), the IHACRES model (Croke and Jakeman, 2004), the GR4J model (Perrin et al., 2003), and many others. These or similar models have been applied to many catchments in the UK by various authors (e.g. Smith et al., 2019; Lane et al., 2019; Coxon et al., 2019). The seasonal signatures suggest that for most of the catchments, particularly if they are not underlain by a highly productive aquifer, a parallel model structure is a reasonable choice (at least for reproducing the response to seasonal forcing). For some groundwater-dominated catchments, however, the fast flow component seems to be rather unimportant. Many of these catchments, typically catchments underlain by Chalk, could only be poorly modelled in national-scale modelling studies (Smith et al., 2019; Lane et al., 2019; Coxon et al., 2019). While this might partly be due to water balance problems (inter-catchment groundwater flows), it might also be due to an inadequate model structure or inadequate parameter ranges. The most parsimonious reservoir configuration to explain the seasonal behaviour of these catchments (phase shifts > 91 days) would be two reservoirs in series, e.g. a soil or unsaturated zone reservoir transforming the incoming forcing into recharge, and a (linear) groundwater reservoir. At least one of these reservoirs would need to be very slow to obtain such large phase shifts (cf. Figure 2). For these groundwater-dominated catchments, a serial structure as it is also used in simple lumped groundwater models (e.g. Peters et al., 2003; Obergfell et al., 2019), seems to be a reasonable choice (at least for reproducing the response to seasonal forcing). As mentioned before, two reservoirs in parallel and two reservoirs in series, respectively, might be seen as "special cases" of a soil reservoir followed by a fast and a slow reservoir. For example, some of the catchments underlain by a highly productive aquifer fall in the area that can be simulated by two reservoirs in parallel (see Figure 6d). Their large phase shifts and their proximity to the "single reservoir line" suggest, however, that the slow flow component is of particular importance and that large time constants (> 100 days) are required to model their behaviour.

In summary, the first control on the attenuation of the seasonal signal in the UK is the partitioning between fast flow and slow flow. More saturated catchments partition more rainfall into fast flow and hence lead to a higher amplitude ratio and to a smaller phase shift. The second control are catchment subsurface properties, which determine the available storage and how slowly water leaves the system. The slower the catchment responds, the larger the phase shift and the lower the amplitude ratio. The Chalk catchments in the UK might be seen as an extreme case where almost all the water infiltrates, and hence the response time of a single slow reservoir (or perhaps two reservoirs in series) is the main control on the propagation of a periodic signal. On the other end of the spectrum, there are fully saturated, very responsive catchments mostly along the west coast of the UK, which behave almost like a single fast reservoir. Using conceptual reservoirs is only one way to interpret the seasonal

signatures. It is useful as many hydrological models are built in that way. There might be, however, other possible ways of  
465 interpretation which we do not consider here.

### 5.3 A hydro-meteorologically more diverse set of catchments – the contiguous US

From Figure 7 and Table 3 it can be seen that for CAMELS catchments (US) the climate indices explain most of the variability  
in the seasonal response. Again, more humid catchments tend to create more fast flow, and hence they have high amplitude  
ratios and small phase shifts. Catchments with a larger moisture index seasonality tend to have smaller phase shifts. In these  
470 catchments precipitation and potential evapotranspiration are mostly out of phase. Therefore, precipitation falls in more humid  
months, which might lead to a flashier response. That means that both precipitation falling on wetter catchments and precip-  
itation falling in wetter months will be attenuated less. The influence of catchment form is much less pronounced than in the  
climatically more homogeneous UK. Continental or global studies tend to identify climate as the dominant hydrological driv-  
ing force (van Dijk, 2010; Beck et al., 2015), yet regional studies often show other attributes such as geology to be important  
475 (for baseflow, see e.g. Longobardi and Villani, 2008; Bloomfield et al., 2009). Our findings highlight anew that generalising  
from global to regional scale, or from regional to global scale, is not straightforward. Such scaling should ideally be done  
in a process-based way, or by analysing sub-climates, as the dominance of climate might mask the influence of other factors  
at large scales. We can also see that the attribute "fraction of highly productive fractured aquifers" (Figure 6d), which is a  
hydrogeological classification available for the UK, shows a much clearer pattern than any soil or geology attributes in the US  
480 (see e.g. Figure 7d which shows the fraction of carbonate sedimentary rock; the same is true if we use e.g. soil permeability for  
the UK). This might partly be due to the more heterogeneous US climate which masks the influence of subsurface properties  
to some degree. But it might also indicate that the soil or geology data used do not contain the hydrologically relevant soil  
or geology information. The hydrogeological classification based on expert judgement available for the UK, even though it is  
only categorical, might be more representative of the actual hydro(geo)logical processes at the scale of interest. We therefore  
485 cannot conclude that in the US catchment form does not play a role. We can merely say that the catchment attributes used do  
not show clear patterns at the continental scale.

Some of the rather arid catchments in the US plot outside the area that can be modelled by two reservoirs in series or in  
parallel (Figure 7). This either indicates that we would need another reservoir in series to model the observed phase shift  
(three reservoirs in series would result in a maximum phase shift of approximately 273 days), that (linear) reservoirs are not a  
490 good description of the hydrological processes, or that the proposed signatures are unreliable for these arid catchments. Since in  
water-limited catchments, actual evapotranspiration is typically much smaller than potential evapotranspiration, the input signal  
we use is very likely a poor proxy for the actual input signal. In very arid catchments ( $I_m < -0.5$ , dark red dots in Figure 7a),  
particularly with low moisture seasonality index (Figure 7b), the results should therefore be interpreted with care. It is unclear  
to what extent these large phase shifts are the result of a poorly approximated input signal or actual catchment function. This  
495 compromises the consistency (McMillan et al., 2017) of the seasonal signatures and makes them most suitable for energy-  
limited catchments. A way to overcome this limitation would be the use of modelled or measured actual evapotranspiration as

input data. As this would require another modelling step or additional data, we leave this for future work (see Supplement for further information).

#### 5.4 Can two common hydrological models reproduce the observed seasonal signatures?

500 The ensemble of IHACRES simulations covers the observed range of amplitude ratios and phase shifts, although one catchment sits just at the boundary of the point cloud (Figure 8a, Figures 9a-c). The BFI pattern also roughly resembles the observed pattern (Figure 6c). Catchments with low BFIs tend to have high amplitude ratios and small phase shifts and vice versa. To explain the signature space of IHACRES, it is useful to recall the structure of the model. IHACRES consists of a soil moisture deficit store, followed by two parallel linear reservoirs. It thus approximately features the two examples introduced in Section 2, namely two reservoirs in series or in parallel.

If one of the parallel reservoirs in IHACRES receives very little water (due to an extremely high or low fraction  $p$  going into the slow reservoir), the whole system acts like two reservoirs in series. The only difference is that the first reservoir is not a single linear reservoir. It is a non-linear deficit store and thus different from the idealised linear reservoir. This might explain why the upper boundary looks similar to the grey dashed line indicating two linear reservoirs in series, yet not exactly the same.

510 We did explore how non-linear reservoirs behave in terms of amplitude ratio and phase shift and they seem to behave similar to linear reservoirs (see Supplement). Another reason for IHACRES not covering the whole area might be the parameters ranges (see Supplement for details). The parameters ranges used are intended to be wide, yet especially the fast reservoir is (to be indeed fast) limited to 10 days, which limits the theoretical space to be smaller than shown in Figure 2.

If the soil moisture reservoir transmits water relatively quickly without much attenuation, the whole system acts like two 515 reservoirs in parallel. In summary, IHACRES is very similar to the idealised arrangement we introduced in Section 2 and this can be seen in the model output. It is therefore likely that IHACRES is capable of reproducing the observed seasonal signatures for catchments in the UK (Figure 6) and for most of the catchments in the US (Figure 7). Whether IHACRES can reproduce the seasonal signatures, other hydrological signatures and achieve satisfactory statistical performance metrics simultaneously is to be explored and beyond the scope of this paper.

520 The ensemble of GR4J simulations covers most of the amplitude ratios and phase shifts observed in the UK (Figure 8b, Figures 9d-f). Many of the model runs lead to amplitude ratios higher than unity, which is caused by the groundwater exchange parameter, which allows the model to import water in addition to incoming  $P$ . While this is possible (and can in fact be observed; e.g. in Figure 6c the blue dot outside the grey boundaries is a catchment with water transfer from a neighbouring catchment), it is observed very rarely in the catchments investigated. Furthermore, a non-zero groundwater exchange parameter 525 should ideally be associated with actual water inputs or outputs (e.g. inter-catchment groundwater flows), and these inputs or outputs are usually unknown. It is worth noting that many model runs that lead to signature values at the boundaries of the signature space (e.g. low BFIs or large phase shifts) are associated with large (positive or negative) values for the groundwater exchange parameter (not shown here). This might further reduce the "realistic" signature space, as, for example, obtaining a low amplitude ratio by removing water might be seen as "the right answer for the wrong reason". No model run leads to a 530 phase shift larger than about 110 days. GR4J also has a soil moisture store followed by two parallel routing stores, i.e. the



overall model structure is similar to IHACRES. The stores are, however, not linear reservoirs. In addition to that, GR4J has fixed internal parameter values, such as the fraction of water going through the slow routing store, which is set to 0.9. This might explain why the BFI tends to be very high, as it can be seen from Figure 9f. Despite the tendency towards large BFIs, GR4J cannot produce phase shifts larger than about 110 days given the parameter ranges used here. This might be due to a too narrow range of the flow delay parameter (maximum 15 d). So, to model both the phase shift and the BFI correctly, we might require a more flexible splitting between fast and slow routing and a means to produce larger phase shifts (e.g. via a wider range for the flow delay parameter).

Figure 9 also shows how the seasonal signatures (and the BFI) vary with different input (forcing). For both models, more humid catchments lead to higher amplitude ratios and smaller phase shifts, and vice versa. This trend, not necessarily the values themselves, agrees with the observed behaviour shown in Figures 6a and 7a.

This analysis is necessarily incomplete for (at least) two reasons. First, we only looked at 40 catchments in the UK to limit the computational demand. Therefore, the conclusions are not necessarily transferable to catchments outside the UK. More arid catchments (e.g. in the US) might show a different behaviour (e.g. the catchments showing phase shifts larger than 182 days, see Figure 7). Second, the sampling scheme (Latin Hypercube sampling) explores only a subspace of the actual parameter values (both because of the parameter ranges and because of the finite amount of parameter sets). We also made an a-priori decision of how to sample by choosing Latin Hypercube sampling in the first place. This is inevitably subjective, and other sampling schemes might lead to different results. This might especially affect the distributions of the modelled signatures shown in Figure 9. Wider parameter ranges might change the ranges of the resulting signature spaces. As we use rather wide ranges based on recent literature (see Supplement for details), our results should (at least) be representative of current modelling practice. This kind of analysis and the seasonal signatures can therefore help to select (or not select) models a-priori, without calibrating them to streamflow data (cf. Vogel and Sankarasubramanian, 2003). This might be particularly helpful for large sample studies where often a certain model structure is chosen a-priori, even if it might be inadequate for the catchment sample investigated (Addor and Melsen, 2019).

## 6 Conclusions and outlook

We have tested seasonal hydrological signatures aimed at representing how climate seasonality is translated into streamflow seasonality, both approximated by sine waves. The damping (the amplitude ratio) and the phase shift of the incoming sine wave have been used to quantify how catchments respond to seasonal forcing. The presented signatures follow the guidelines of McMillan et al. (2017). The signatures are identifiable, robust, and consistent (see Supplement for further information). They are representative and have discriminatory power as they exhibit explicable, hydrologically interpretable patterns, particularly for energy-limited catchments (Figures 6 and 7). They can be related to conceptual model structures (arrangements of linear reservoirs, Figure 5), and the model evaluation (Figure 8) has shown that we can indeed observe this theoretical behaviour in model outputs. As we use precipitation minus potential evapotranspiration as a proxy for the input to a catchment, the seasonal signatures are unreliable for water-limited catchments. To use the seasonal signatures in water-limited catchments we would

need to estimate actual evapotranspiration. The current approach is therefore only suitable for energy-limited, non-snowy catchments with a distinct unimodal seasonality, such as catchments in the UK.

We have found that the propagation of the seasonal input through a catchment depends both on climate and catchment form. Climate aridity and seasonality, and corresponding annual and seasonal catchment wetness, drive the partitioning of the incoming forcing into fast and slow flow. Catchment form, such as subsurface properties, influences how strongly the seasonal input gets attenuated. This is particularly visible in the UK, where the hydrogeological classification available (fraction of highly productive aquifer) can explain the very slow response of some catchments. The seemingly more dominant (and less clear) role of climate in the US highlights that scaling from regional to continental (or global) scale is not straightforward and requires thoughtful, ideally process-based approaches. Or in the words of Turner (1989), "conclusions or inferences regarding landscape patterns and processes must be drawn with an acute awareness of scale". Nonetheless, the clear link to climate and aquifer characteristics in the UK suggests that the signatures might be useful for catchment classification and for predictions in ungauged catchments, as long as potential evapotranspiration is an adequate proxy for actual evapotranspiration.

The model evaluation has shown that the signatures have the potential to be used as a diagnostic tool. GR4J could not reproduce the observed combinations of phase shift and BFI, pointing towards structural deficiencies of the model for certain catchments. As the seasonal signatures are relatable to conceptual model structures (arrangements of reservoirs), we could – given sufficient data – also build models based on inference from observed values of the signatures, and not just test existing model structures. This could be done in a stepwise fashion, starting with the seasonal time scale and then adding more complexity if needed (Jothityangkoon et al., 2001; Farmer et al., 2003; McMillan et al., 2011). It would be a step towards model structure identification based on hydrological reasoning, i.e. getting the right answers for the right reasons (Kirchner, 2006). If we decide on a certain model structure (e.g. two reservoirs in series), we can then use the presented theory to estimate time constants of the reservoirs (the parameters). This could be used as additional constraint in the calibration process. If the time constants obtained from the seasonal signatures differ from time constants obtained by other means, e.g. by calibrating the model using a metric such as KGE, this might be indicative of limitations of typical modelling approaches (Fowler et al., 2018). It might be that the slower annual signal is exciting different parts of the catchments than events (individual peaks or recessions) do, which we typically calibrate to.

The idea of exploring a model's signature space (following the approach of Vogel and Sankarasubramanian, 2003) perhaps deserves more attention. It allows to explore models systematically and it can reveal whether a model can simulate the ranges of hydrological signatures we obtain by analysing catchment data. Similar to sensitivity analysis, it allows us to explore and to better understand how a model works, which parameters are important for which signature, and what output behaviour a model can generate in general – without (and before) calibration. While we limited this analysis to a few signatures, in future studies we should focus on testing whether a model can simultaneously reproduce multiple signatures focusing on different aspects of the hydrological system (Euser et al., 2013; Hrachowitz et al., 2014).

*Code and data availability.* A repository with Matlab code used for the analysis and the resulting data is available from [https://github.com/SebastianGnann/Seasonal\\_signatures\\_paper\\_public](https://github.com/SebastianGnann/Seasonal_signatures_paper_public). Colours are based on [www.ColorBrewer.org](http://www.ColorBrewer.org), by Cynthia A. Brewer, Penn State. The MARRMoT toolbox is available from <https://github.com/wknoben/MARRMoT>. The CAMELS dataset is available from <https://ral.ucar.edu/solutions/products/camels>. Information about the UK Benchmark Network can be obtained from <https://nrfa.ceh.ac.uk/benchmark-network>.  
600 Streamflow data and catchments attributes are available from <https://nrfa.ceh.ac.uk>. CEH-GEAR precipitation data are available from <https://doi.org/10.5285/33604ea0-c238-4488-813d-0ad9ab7c51ca>. CHESS-PE potential evapotranspiration data are available from <https://doi.org/10.5285/8baf805d-39ce-4dac-b224-c926ada353b7>.

*Author contributions.* SJG, NJKH and RAW conceptualised the research project. SJG performed the formal analysis. SJG prepared the manuscript with contributions from all co-authors.

605 *Competing interests.* The authors declare that they have no conflict of interest.

*Acknowledgements.* This work is funded as part of the Water Informatics Science and Engineering Centre for Doctoral Training (WISE CDT) under a grant from the Engineering and Physical Sciences Research Council (EPSRC), grant number EP/L016214/1. Parts of this work were carried out using the computational facilities of the Advanced Computing Research Centre, University of Bristol - <http://www.bris.ac.uk/acrc/>. Thanks to Wouter Knoben for help with the MARRMoT toolbox, helpful discussions, and for helpful comments on an earlier  
610 version of this manuscript. Thanks to Gemma Coxon for assisting with the data. We also thank the Editor and three anonymous reviewers for their helpful feedback.

## References

- Addor, N. and Melsen, L. A.: Legacy, rather than adequacy, drives the selection of hydrological models, *Water Resources Research*, 55, 378–390, <https://doi.org/10.1029/2018WR022958>, 2019.
- 615 Addor, N., Newman, A. J., Mizukami, N., and Clark, M. P.: The CAMELS data set: catchment attributes and meteorology for large-sample studies, *Hydrology and Earth System Sciences*, 21, 5293–5313, <https://doi.org/10.5194/hess-21-5293-2017>, 2017.
- Addor, N., Nearing, G., Prieto, C., Newman, A. J., Le Vine, N., and Clark, M. P.: A ranking of hydrological signatures based on their predictability in space, *Water Resources Research*, 54, 8792–8812, <https://doi.org/10.1029/2018WR022606>, 2018.
- Beck, H. E., de Roo, A., and van Dijk, A. I. J. M.: Global maps of streamflow characteristics based on observations from several thousand  
620 catchments, *Journal of Hydrometeorology*, 16, 1478–1501, <https://doi.org/10.1175/JHM-D-14-0155.1>, 2015.
- Berghuijs, W. R., Sivapalan, M., Woods, R. A., and Savenije, H. H. G.: Patterns of similarity of seasonal water balances: A window into streamflow variability over a range of time scales, *Water Resources Research*, 50, 5638–5661, <https://doi.org/10.1002/2014WR015692>, 2014.
- Beven, K. J. and Kirkby, M. J.: A physically based, variable contributing area model of basin hydrology, *Hydrological Sciences Bulletin*, 24,  
625 43–69, <https://doi.org/10.1080/02626667909491834>, 1979.
- Bloomfield, J. P., Allen, D. J., and Griffiths, K. J.: Examining geological controls on baseflow index (BFI) using regression analysis: An illustration from the Thames Basin, UK, *Journal of Hydrology*, 373, 164–176, <https://doi.org/10.1016/j.jhydrol.2009.04.025>, 2009.
- Cayan, D. R., Riddle, L. G., and Aguado, E.: The influence of precipitation and temperature on seasonal streamflow in California, *Water Resources Research*, 29, 1127–1140, <https://doi.org/10.1029/92WR02802>, 1993.
- 630 Cheng, J. and Druzdzel, M.: Latin hypercube sampling in Bayesian networks., *Proceedings of the Thirteenth International Florida Artificial Intelligence Research Symposium Conference*, pp. 287–292, <http://www.aaai.org/Papers/FLAIRS/2000/FLAIRS00-054.pdf>, 2000.
- Clausen, B. and Biggs, B.: Flow variables for ecological studies in temperate streams: groupings based on covariance, *Journal of Hydrology*, 237, 184–197, [https://doi.org/10.1016/S0022-1694\(00\)00306-1](https://doi.org/10.1016/S0022-1694(00)00306-1), 2000.
- Colwell, R. K.: Predictability, constancy, and contingency of periodic phenomena, *Ecology*, 55, 1148–1153, <https://doi.org/10.2307/1940366>,  
635 1974.
- Court, A.: Measures of streamflow timing, *Journal of Geophysical Research*, 67, 4335–4339, <https://doi.org/10.1029/JZ067i011p04335>, 1962.
- Coxon, G., Freer, J., Lane, R., Dunne, T., Knoben, W. J. M., Howden, N. J. K., Quinn, N., Wagener, T., and Woods, R.: DE-CIPHeR v1: Dynamic fluxEs and ConnectIvity for Predictions of HydRology, *Geoscientific Model Development*, 12, 2285–2306,  
640 <https://doi.org/10.5194/gmd-12-2285-2019>, 2019.
- Croke, B. F. and Jakeman, A. J.: A catchment moisture deficit module for the IHACRES rainfall-runoff model, *Environmental Modelling and Software*, 19, 1–5, <https://doi.org/10.1016/j.envsoft.2003.09.001>, 2004.
- DeWalle, D. R., Edwards, P. J., Swistock, B. R., Aravena, R., and Drimmie, R. J.: Seasonal isotope hydrology of three Appalachian forest catchments, *Hydrological Processes*, 11, 1895–1906, [https://doi.org/10.1002/\(SICI\)1099-1085\(199712\)11:15<1895::AID-HYP538>3.0.CO;2-%23](https://doi.org/10.1002/(SICI)1099-1085(199712)11:15<1895::AID-HYP538>3.0.CO;2-%23), 1997.  
645
- Dooge, J.: *Linear theory of hydrologic systems*, 1468, Agricultural Research Service, US Department of Agriculture, 1973.
- Eriksson, E.: Compartment models and reservoir theory, *Annual Review of Ecology and Systematics*, 2, 67–84, <https://doi.org/10.1146/annurev.es.02.110171.000435>, 1971.

- Erskine, A. and Papaioannou, A.: The use of aquifer response rate in the assessment of groundwater resources, *Journal of Hydrology*, 202, 373–391, [https://doi.org/10.1016/S0022-1694\(97\)00058-9](https://doi.org/10.1016/S0022-1694(97)00058-9), 1997.
- Euser, T., Winsemius, H. C., Hrachowitz, M., Fenicia, F., Uhlenbrook, S., and Savenije, H. H. G.: A framework to assess the realism of model structures using hydrological signatures, *Hydrology and Earth System Sciences*, 17, 1893–1912, <https://doi.org/10.5194/hess-17-1893-2013>, 2013.
- Farmer, D., Sivapalan, M., and Jothityangkoon, C.: Climate, soil, and vegetation controls upon the variability of water balance in temperate and semiarid landscapes: Downward approach to water balance analysis, *Water Resources Research*, 39, 1–21, <https://doi.org/10.1029/2001WR000328>, 2003.
- Fowler, K., Coxon, G., Freer, J., Peel, M., Wagener, T., Western, A., Woods, R. A., and Zhang, L.: Simulating runoff under changing climatic conditions: a framework for model improvement, *Water Resources Research*, 54, 9812–9832, <https://doi.org/10.1029/2018WR023989>, 2018.
- Gupta, H. V., Wagener, T., and Liu, Y.: Reconciling theory with observations: elements of a diagnostic approach to model evaluation, *Hydrological Processes*, 22, 3802–3813, <https://doi.org/10.1002/hyp.6989>, 2008.
- Gupta, H. V., Kling, H., Yilmaz, K. K., and Martinez, G. F.: Decomposition of the mean squared error and NSE performance criteria: Implications for improving hydrological modelling, *Journal of Hydrology*, 377, 80–91, <https://doi.org/10.1016/j.jhydrol.2009.08.003>, 2009.
- Harman, C. J.: Age-ranked storage-discharge relations – a unified description of spatially-lumped flow and water age in hydrologic systems, *Water Resources Research*, p. 2017WR022304, <https://doi.org/10.1029/2017WR022304>, 2019.
- Harrigan, S., Hannaford, J., Muchan, K., and Marsh, T. J.: Designation and trend analysis of the updated UK Benchmark Network of river flow stations: the UKBN2 dataset, *Hydrology Research*, 49, 552–567, <https://doi.org/10.2166/nh.2017.058>, 2018a.
- Harrigan, S., Prudhomme, C., Parry, S., Smith, K., and Tanguy, M.: Benchmarking ensemble streamflow prediction skill in the UK, *Hydrology and Earth System Sciences*, 22, 2023–2039, <https://doi.org/10.5194/hess-22-2023-2018>, 2018b.
- Hrachowitz, M., Savenije, H., Blöschl, G., McDonnell, J., Sivapalan, M., Pomeroy, J., Arheimer, B., Blume, T., Clark, M., Ehret, U., Fenicia, F., Freer, J., Gelfan, A., Gupta, H., Hughes, D., Hut, R., Montanari, A., Pande, S., Tetzlaff, D., Troch, P., Uhlenbrook, S., Wagener, T., Winsemius, H., Woods, R., Zehe, E., and Cudennec, C.: A decade of Predictions in Ungauged Basins (PUB) – a review, *Hydrological Sciences Journal*, 58, 1198–1255, <https://doi.org/10.1080/02626667.2013.803183>, 2013.
- Hrachowitz, M., Fovet, O., Ruiz, L., Euser, T., Gharari, S., Nijzink, R., Freer, J., Savenije, H. H. G., and Gascuel-Oudou, C.: Process consistency in models: The importance of system signatures, expert knowledge, and process complexity, *Water Resources Research*, 50, 7445–7469, <https://doi.org/10.1002/2014WR015484>, 2014.
- Institute of Hydrology: Low Flow Studies Report No. 1: Research Report, Institute of Hydrology, 1980.
- Jasechko, S., Birks, S. J., Gleeson, T., Wada, Y., Fawcett, P. J., Sharp, Z. D., McDonnell, J. J., and Welker, J. M.: The pronounced seasonality of global groundwater recharge, *Water Resources Research*, 50, 8845–8867, <https://doi.org/10.1002/2014WR015809>, 2014.
- Jothityangkoon, C., Sivapalan, M., and Farmer, D.: Process controls of water balance variability in a large semi-arid catchment: downward approach to hydrological model development, *Journal of Hydrology*, 254, 174–198, [https://doi.org/10.1016/S0022-1694\(01\)00496-6](https://doi.org/10.1016/S0022-1694(01)00496-6), 2001.
- Kirchner, J. W.: Getting the right answers for the right reasons: Linking measurements, analyses, and models to advance the science of hydrology, *Water Resources Research*, 42, 1–5, <https://doi.org/10.1029/2005WR004362>, 2006.
- Kirchner, J. W.: Aggregation in environmental systems – Part 1: Seasonal tracer cycles quantify young water fractions, but not mean transit times, in spatially heterogeneous catchments, *Hydrology and Earth System Sciences*, 20, 279–297, <https://doi.org/10.5194/hess-20-279-2016>, 2016.

- Knoben, W. J. M., Woods, R. A., and Freer, J. E.: A quantitative hydrological climate classification evaluated with independent streamflow data, *Water Resources Research*, 54, 5088–5109, <https://doi.org/10.1029/2018WR022913>, 2018.
- Knoben, W. J. M., Freer, J. E., Fowler, K. J. A., Peel, M. C., and Woods, R. A.: Modular Assessment of Rainfall–Runoff Models Toolbox (MARRMoT) v1.2: an open-source, extendable framework providing implementations of 46 conceptual hydrologic models as continuous state-space formulations, *Geoscientific Model Development*, 12, 2463–2480, <https://doi.org/10.5194/gmd-12-2463-2019>, 2019a.
- Knoben, W. J. M., Woods, R. A., and Freer, J. E.: Global bimodal precipitation seasonality: A systematic overview, *International Journal of Climatology*, 39, 558–567, <https://doi.org/10.1002/joc.5786>, 2019b.
- Laaha, G. and Blöschl, G.: Seasonality indices for regionalizing low flows, *Hydrological Processes*, 20, 3851–3878, <https://doi.org/10.1002/hyp.6161>, 2006.
- Laaha, G., Demuth, S., Hisdal, H., Kroll, C. N., van Lanen, H. A. J., Nester, T., Rogger, M., Sauquet, E., Tallaksen, L. M., Woods, R. A., and Young, A.: Prediction of low flows in ungauged basins, in: *Runoff Prediction in Ungauged Basins*, edited by Blöschl, G., Sivapalan, M., Wagener, T., Viglione, A., and Savenije, H., 2011, pp. 163–188, Cambridge University Press, Cambridge, <https://doi.org/10.1017/CBO9781139235761.011>, 2013.
- Lane, R. A., Coxon, G., Freer, J. E., Wagener, T., Johnes, P. J., Bloomfield, J. P., Greene, S., Macleod, C. J. A., and Reaney, S. M.: Benchmarking the predictive capability of hydrological models for river flow and flood peak predictions across over 1000 catchments in Great Britain, *Hydrology and Earth System Sciences*, 23, 4011–4032, <https://doi.org/10.5194/hess-23-4011-2019>, <https://www.hydrol-earth-syst-sci.net/23/4011/2019/>, 2019.
- Longobardi, A. and Villani, P.: Baseflow index regionalization analysis in a Mediterranean area and data scarcity context: Role of the catchment permeability index, *Journal of Hydrology*, 355, 63–75, <https://doi.org/10.1016/j.jhydrol.2008.03.011>, 2008.
- McGuire, K. J. and McDonnell, J. J.: A review and evaluation of catchment transit time modeling, *Journal of Hydrology*, 330, 543–563, <https://doi.org/10.1016/j.jhydrol.2006.04.020>, 2006.
- McMillan, H., Westerberg, I., and Branger, F.: Five guidelines for selecting hydrological signatures, *Hydrological Processes*, 31, 4757–4761, <https://doi.org/10.1002/hyp.11300>, 2017.
- McMillan, H. K., Clark, M. P., Bowden, W. B., Duncan, M., and Woods, R. A.: Hydrological field data from a modeller’s perspective: Part 1. Diagnostic tests for model structure, *Hydrological Processes*, 25, 511–522, <https://doi.org/10.1002/hyp.7841>, 2011.
- McMillan, H. K., Gueguen, M., Grimon, E., Woods, R. A., Clark, M. P., and Rupp, D. E.: Spatial variability of hydrological processes and model structure diagnostics in a 50km<sup>2</sup> catchment, *Hydrological Processes*, 28, 4896–4913, <https://doi.org/10.1002/hyp.9988>, 2014.
- Milly, P. C. D.: Climate, soil water storage, and the average annual water balance, *Water Resources Research*, 30, 2143–2156, <https://doi.org/10.1029/94WR00586>, 1994.
- Montanari, A. and Toth, E.: Calibration of hydrological models in the spectral domain: An opportunity for scarcely gauged basins?, *Water Resources Research*, 43, 1–10, <https://doi.org/10.1029/2006WR005184>, 2007.
- Moore, R. J.: The PDM rainfall-runoff model, *Hydrology and Earth System Sciences*, 11, 483–499, <https://doi.org/10.5194/hess-11-483-2007>, 2007.
- Nash, J.: The form of the instantaneous unit hydrograph, *International Association of Scientific Hydrology, Publ*, 3, 114–121, 1957.
- Nash, J. and Sutcliffe, J.: River flow forecasting through conceptual models part I – A discussion of principles, *Journal of Hydrology*, 10, 282–290, [https://doi.org/10.1016/0022-1694\(70\)90255-6](https://doi.org/10.1016/0022-1694(70)90255-6), 1970.
- National River Flow Archive: <https://nrfa.ceh.ac.uk>, NERC CEH, Wallingford, <https://nrfa.ceh.ac.uk>, 2019.

- Newman, A. J., Clark, M. P., Sampson, K., Wood, A., Hay, L. E., Bock, A., Viger, R. J., Blodgett, D., Brekke, L., Arnold, J. R., Hopson, T., and Duan, Q.: Development of a large-sample watershed-scale hydrometeorological data set for the contiguous USA: data set characteristics and assessment of regional variability in hydrologic model performance, *Hydrology and Earth System Sciences*, 19, 209–223, <https://doi.org/10.5194/hess-19-209-2015>, 2015.
- Oberghell, C., Bakker, M., and Maas, K.: Estimation of average diffuse aquifer recharge using time series modeling of groundwater heads, *Water Resources Research*, 55, 2194–2210, <https://doi.org/10.1029/2018WR024235>, 2019.
- Olden, J. D. and Poff, N. L.: Redundancy and the choice of hydrologic indices for characterizing streamflow regimes, *River Research and Applications*, 19, 101–121, <https://doi.org/10.1002/rra.700>, 2003.
- Oudin, L., Salavati, B., Furusho-Percot, C., Ribstein, P., and Saadi, M.: Hydrological impacts of urbanization at the catchment scale, *Journal of Hydrology*, 559, 774–786, <https://doi.org/10.1016/j.jhydrol.2018.02.064>, 2018.
- Peel, M. C. and Blöschl, G.: Hydrological modelling in a changing world, *Progress in Physical Geography*, 35, 249–261, <https://doi.org/10.1177/0309133311402550>, 2011.
- Perrin, C., Michel, C., and Andréassian, V.: Improvement of a parsimonious model for streamflow simulation, *Journal of Hydrology*, 279, 275–289, [https://doi.org/10.1016/S0022-1694\(03\)00225-7](https://doi.org/10.1016/S0022-1694(03)00225-7), 2003.
- Peters, E., Torfs, P. J., van Lanen, H. A., and Bier, G.: Propagation of drought through groundwater – A new approach using linear reservoir theory, *Hydrological Processes*, 17, 3023–3040, <https://doi.org/10.1002/hyp.1274>, 2003.
- Poff, N. L. and Zimmerman, J. K. H.: Ecological responses to altered flow regimes: a literature review to inform the science and management of environmental flows, *Freshwater Biology*, 55, 194–205, <https://doi.org/10.1111/j.1365-2427.2009.02272.x>, 2010.
- Poff, N. L., Allan, J. D., Bain, M. B., Karr, J. R., Prestegard, K. L., Richter, B. D., Sparks, R. E., and Stromberg, J. C.: The Natural Flow Regime, *BioScience*, 47, 769–784, <https://doi.org/10.2307/1313099>, 1997.
- Post, D. A. and Jakeman, A. J.: Predicting the daily streamflow of ungauged catchments in S.E. Australia by regionalising the parameters of a lumped conceptual rainfall-runoff model, *Ecological Modelling*, 123, 91–104, [https://doi.org/10.1016/S0304-3800\(99\)00125-8](https://doi.org/10.1016/S0304-3800(99)00125-8), 1999.
- Regonda, S. K., Rajagopalan, B., Clark, M., and Pitlick, J.: Seasonal cycle shifts in hydroclimatology over the western United States, *Journal of Climate*, 18, 372–384, <https://doi.org/10.1175/JCLI-3272.1>, 2005.
- Richter, B. D., Baumgartner, J. V., Powell, J., and Braun, D. P.: A method for assessing hydrologic alteration within ecosystems, *Conservation Biology*, 10, 1163–1174, <https://doi.org/10.1046/j.1523-1739.1996.10041163.x>, 1996.
- Robinson, E., Blyth, E., Clark, D., Comyn-Platt, E., Finch, J., and Rudd, A.: Climate hydrology and ecology research support system potential evapotranspiration dataset for Great Britain (1961-2015) [CHESS-PE], <https://doi.org/10.5285/8baf805d-39ce-4dac-b224-c926ada353b7>, 2016.
- Sawicz, K., Wagener, T., Sivapalan, M., Troch, P. A., and Carrillo, G.: Catchment classification: Empirical analysis of hydrologic similarity based on catchment function in the eastern USA, *Hydrology and Earth System Sciences*, 15, 2895–2911, <https://doi.org/10.5194/hess-15-2895-2011>, 2011.
- Schaefli, B.: Snow hydrology signatures for model identification within a limits-of-acceptability approach, *Hydrological Processes*, 30, 4019–4035, <https://doi.org/10.1002/hyp.10972>, 2016.
- Sefton, C. and Howarth, S.: Relationships between dynamic response characteristics and physical descriptors of catchments in England and Wales, *Journal of Hydrology*, 211, 1–16, [https://doi.org/10.1016/S0022-1694\(98\)00163-2](https://doi.org/10.1016/S0022-1694(98)00163-2), 1998.
- Shafii, M. and Tolson, B. A.: Optimizing hydrological consistency by incorporating hydrological signatures into model calibration objectives, *Water Resources Research*, 51, 3796–3814, <https://doi.org/10.1002/2014WR016520>, 2015.

- Shi, X., Wood, A. W., and Lettenmaier, D. P.: How essential is hydrologic model calibration to seasonal streamflow forecasting?, *Journal of Hydrometeorology*, 9, 1350–1363, <https://doi.org/10.1175/2008JHM1001.1>, 2008.
- Smakhtin, V.: Low flow hydrology: a review, *Journal of Hydrology*, 240, 147–186, [https://doi.org/10.1016/S0022-1694\(00\)00340-1](https://doi.org/10.1016/S0022-1694(00)00340-1), 2001.
- 765 Smith, K. A., Barker, L. J., Tanguy, M., Parry, S., Harrigan, S., Legg, T. P., Prudhomme, C., and Hannaford, J.: A multi-objective ensemble approach to hydrological modelling in the UK: an application to historic drought reconstruction, *Hydrology and Earth System Sciences*, 23, 3247–3268, <https://doi.org/10.5194/hess-23-3247-2019>, 2019.
- Svensson, C.: Seasonal river flow forecasts for the United Kingdom using persistence and historical analogues, *Hydrological Sciences Journal*, 61, 19–35, <https://doi.org/10.1080/02626667.2014.992788>, 2016.
- 770 Tanguy, M., Dixon, H., Prosdociimi, I., Morris, D. G., and Keller, V. D. J.: Gridded estimates of daily and monthly areal rainfall for the United Kingdom (1890–2015) [CEH-GEAR], <https://doi.org/10.5285/33604ea0-c238-4488-813d-0ad9ab7c51ca>, 2016.
- Townley, L. R.: The response of aquifers to periodic forcing, *Advances in Water Resources*, 18, 125–146, [https://doi.org/10.1016/0309-1708\(95\)00008-7](https://doi.org/10.1016/0309-1708(95)00008-7), 1995.
- Turner, M. G.: Landscape ecology: the effect of pattern on process, *Annual Review of Ecology and Systematics*, 20, 171–197, <https://doi.org/10.1146/annurev.es.20.110189.001131>, 1989.
- 775 van Dijk, A. I. J. M.: Climate and terrain factors explaining streamflow response and recession in Australian catchments, *Hydrology and Earth System Sciences*, 14, 159–169, <https://doi.org/10.5194/hess-14-159-2010>, 2010.
- Vega, M., Pardo, R., Barrado, E., and Debán, L.: Assessment of seasonal and polluting effects on the quality of river water by exploratory data analysis, *Water Research*, 32, 3581–3592, [https://doi.org/10.1016/S0043-1354\(98\)00138-9](https://doi.org/10.1016/S0043-1354(98)00138-9), 1998.
- 780 Vogel, R. M. and Sankarasubramanian, A.: Validation of a watershed model without calibration, *Water Resources Research*, 39, 1–9, <https://doi.org/10.1029/2002WR001940>, 2003.
- Wagener, T., Sivapalan, M., Troch, P., and Woods, R.: Catchment classification and hydrologic similarity, *Geography Compass*, 1, 901–931, <https://doi.org/10.1111/j.1749-8198.2007.00039.x>, 2007.
- Weingartner, R., Blöschl, G., Hannah, D. M., Marks, D. G., Parajka, J., Pearson, C. S., Rogger, M., Salinas, J. L., Sauquet, E., Srikanthan, R., Thompson, S. E., and Viglione, A.: Prediction of seasonal runoff in ungauged basins, in: *Runoff Prediction in Ungauged Basins*, edited by Blöschl, G., Sivapalan, M., Wagener, T., Viglione, A., and Savenije, H., 2011, pp. 102–134, Cambridge University Press, Cambridge, <https://doi.org/10.1017/CBO9781139235761.009>, 2013.
- 785 Westerberg, I. K., Wagener, T., Coxon, G., McMillan, H. K., Castellarin, A., Montanari, A., and Freer, J.: Uncertainty in hydrological signatures for gauged and ungauged catchments, *Water Resources Research*, 52, 1847–1865, <https://doi.org/10.1002/2015WR017635>, 2016.
- 790 Yadav, M., Wagener, T., and Gupta, H. V.: Regionalization of constraints on expected watershed response behavior for improved predictions in ungauged basins, *Advances in Water Resources*, 30, 1756–1774, <https://doi.org/10.1016/j.advwatres.2007.01.005>, 2007.
- Yokoo, Y. and Sivapalan, M.: Towards reconstruction of the flow duration curve: Development of a conceptual framework with a physical basis, *Hydrology and Earth System Sciences*, 15, 2805–2819, <https://doi.org/10.5194/hess-15-2805-2011>, 2011.
- 795 Young, P.: Data-based mechanistic modelling of environmental, ecological, economic and engineering systems, *Environmental Modelling and Software*, 13, 105–122, [https://doi.org/10.1016/S1364-8152\(98\)00011-5](https://doi.org/10.1016/S1364-8152(98)00011-5), 1998.